Novel Tools for Quantifying Coronary Stenosis: Angio-Imaging vs. CT Approaches

Yoshinobu Onuma, MD. PhD.,
Asahi Oshima, MD., Akihiro Tobe, MD.,
Patrick W. Serruys, MD, PhD.

University of Galway, Ireland
CORRIB Research Centre for Advanced Imaging and Core laboratory

Disclosure

- **The authors have no financial conflicts of interest to disclose concerning the presentation.**

Angio-imaging vs. CTCA

Angiography

CTCA

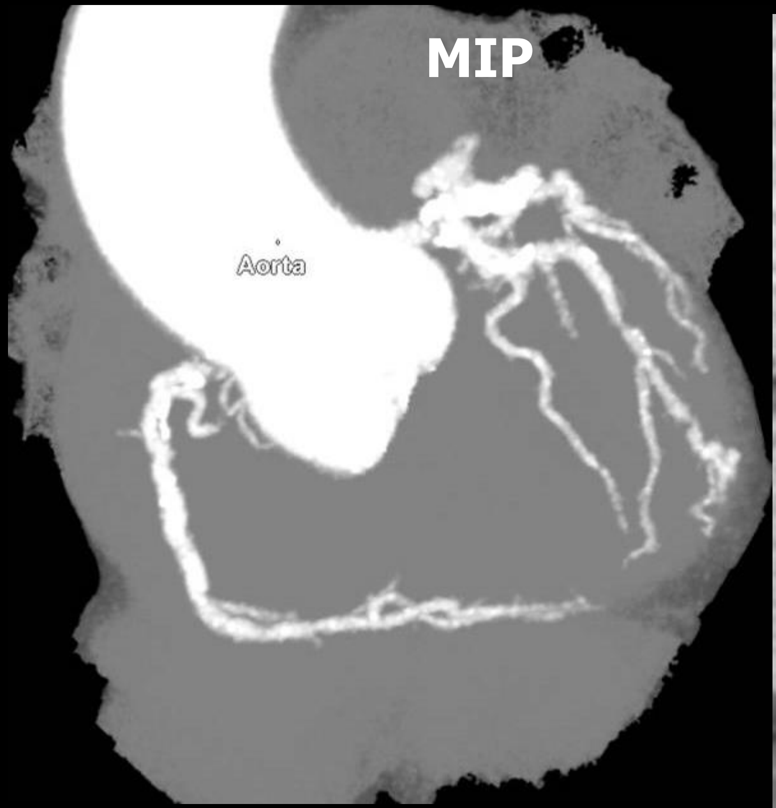

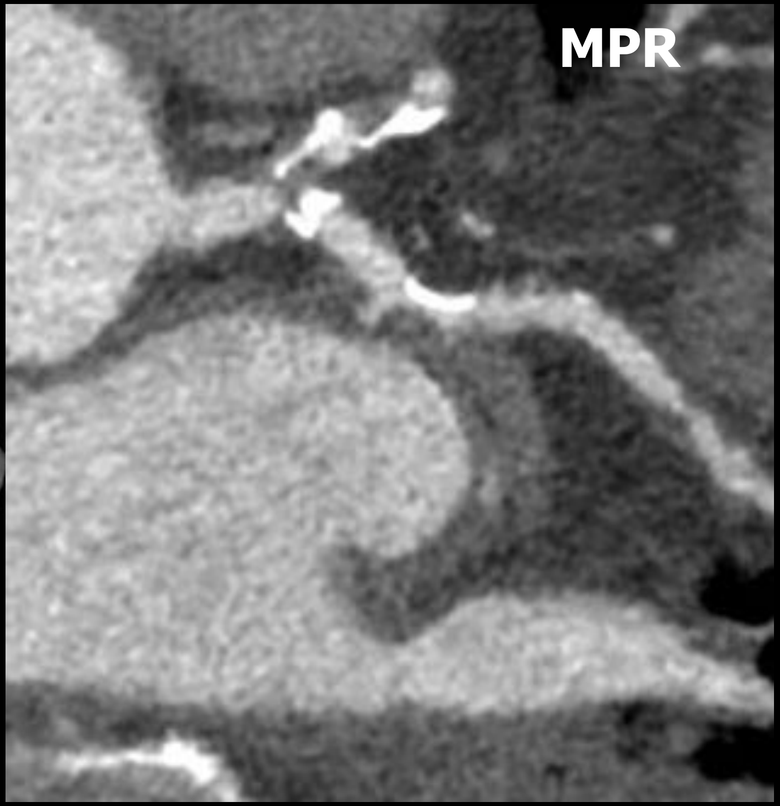

Applying the Artificial intelligence (AI), in coronary angiography

- **Coronary angiography is the gold standard for diagnosis and management decision in coronary artery disease.**

- **However, accurately interpreting coronary angiography requires extensive training and can be subjective due to challenges like multiple viewing angles, dynamic images, overlapping structures, and uneven contrast enhancement.**

- **A more standardized, reproducible approach to angiogram interpretation and coronary stenosis assessment would have clinical importance.**

- **Artificial intelligence (AI),encompassing machine learning (ML) is a computer science dedicated to the development of computational systems capable of performing tasks that traditionally necessitate human intelligence.**

- **AI algorithms are now demonstrating the ability to automate important clinical tasks in interventional cardiology.**

npj Digital Medicine 2023 Vol. 6 Issue 1

Scientific Data 2024 Vol. 11 Issue 1

Training and validation of a deep learning architecture for the automatic analysis of coronary angiography

Tianming Du[1], PhD; Lihua Xie[2], MSc; Honggang Zhang[1], PhD; Xuqing Liu[1], PhD; Xiaofei Wang[3], MSE; Donghao Chen[3], MSE; Yang Xu[3], BSE; Zhongwei Sun[2], MSc; Wenhui Zhou[3], PhD; Lei Song[2], MD; Changdong Guan[2], MSc; Alexandra J. Lansky[4], MD; Bo Xu[2]*, MBBS

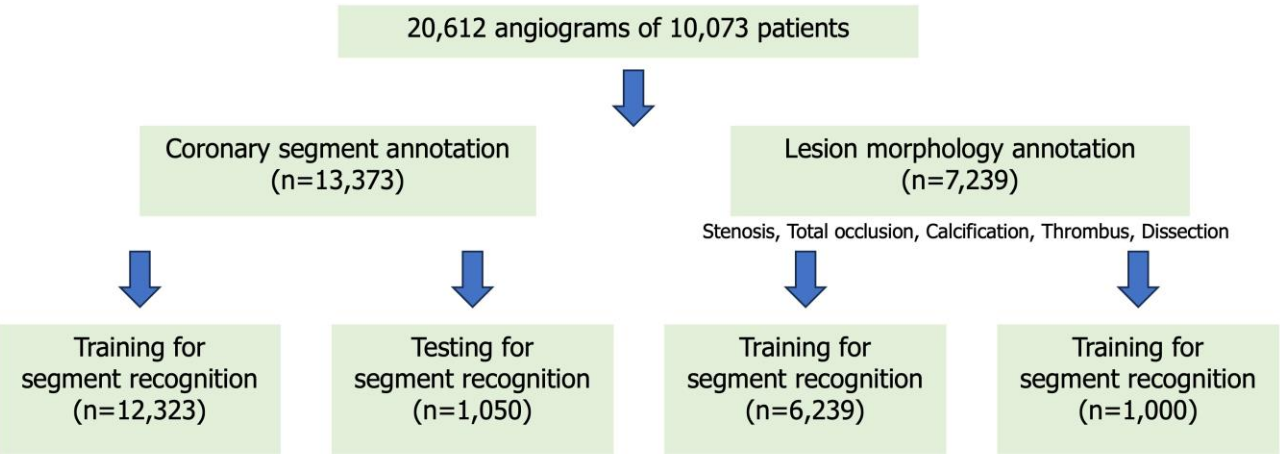

Table 2. Performance of DeepDiscern segment recognition DNN for different coronary artery segments.

Coronary artery segment	Accuracy % (95% CI)	Sensitivity % (95% CI)	Specificity % (95% CI)	PPV % (95% CI)	NPV % (95% CI)
All segments	98.4 (98.3-98.4)	85.2 (84.8-85.6)	99.1 (99.1-99.1)	76.2 (75.7-76.6)	99.5 (99.5-99.5)
LM	99.9 (99.9-99.9)	91.8 (91.1-92.5)	99.9 (99.9-99.9)	80.7 (79.4-82.0)	99.9 (99.9-99.9)
LAD proximal	99.8 (99.8-99.8)	92.6 (91.9-93.2)	99.9 (99.8-99.9)	80.9 (79.5-82.4)	99.9 (99.9-99.9)
LAD mid	99.8 (99.7-99.8)	90.8 (90.1-91.4)	99.8 (99.8-99.8)	82.1 (81.0-83.2)	99.9 (99.9-99.9)
LAD apical	99.7 (99.7-99.7)	84.5 (83.0-86.1)	99.8 (99.8-99.8)	67.8 (66.1-69.5)	99.9 (99.9-99.9)
1st DIA	99.4 (99.4-99.5)	78.1 (75.9-80.4)	99.6 (99.6-99.6)	60.0 (58.1-62.0)	99.8 (99.8-99.9)
2nd DIA	99.7 (99.7-99.8)	73.7 (68.0-79.3)	99.8 (99.8-99.8)	41.2 (36.5-45.9)	99.9 (99.9-99.9)
LCX proximal	99.8 (99.8-99.8)	87.9 (86.4-89.4)	99.9 (99.9-99.9)	78.8 (77.1-80.5)	99.9 (99.9-99.9)
LCX distal	99.7 (99.6-99.7)	81.3 (79.6-83.1)	99.8 (99.8-99.8)	78.3 (76.3-80.2)	99.9 (99.8-99.9)
Intermediate	99.6 (99.5-99.6)	74.1 (69.8-78.4)	99.7 (99.7-99.8)	63.2 (58.1-68.4)	99.9 (99.8-99.9)
OM	99.7 (99.6-99.7)	79.2 (75.9-82.5)	99.8 (99.7-99.8)	53.0 (48.8-57.2)	99.9 (99.9-99.9)
L-PLA	99.5 (99.5-99.5)	80.6 (78.3-82.8)	99.7 (99.6-99.7)	69.1 (66.7-71.4)	99.8 (99.8-99.9)
L-PDA	99.6 (99.5-99.7)	83.1 (79.6-86.6)	99.7 (99.7-99.8)	72.5 (69.1-75.9)	99.9 (99.9-99.9)
RCA proximal	99.8 (99.8-99.8)	87.9 (87.0-88.8)	99.9 (99.9-99.9)	86.7 (85.9-87.5)	99.9 (99.9-99.9)
RCA mid	99.7 (99.7-99.8)	85.6 (84.5-86.7)	99.8 (99.8-99.9)	76.6 (75.3-77.9)	99.9 (99.9-99.9)
RCA distal	99.8 (99.8-99.8)	83.2 (82.0-84.4)	99.9 (99.9-99.9)	88.2 (87.1-89.3)	99.9 (99.9-99.9)
PDA	99.7 (99.7-99.7)	75.4 (73.4-77.4)	99.8 (99.8-99.9)	70.6 (68.7-72.5)	99.9 (99.9-99.9)
PLA	99.5 (99.5-99.5)	77.2 (75.6-78.7)	99.7 (99.7-99.7)	72.0 (70.3-73.7)	99.8 (99.8-99.8)

CI: confidence interval; DIA: diagonal; LAD: left anterior descending artery; LCX: left circumflex artery; LM: left main; L-PDA: left posterior descending; L-PLA: left posterolateral; NPV: negative predictive value; OM: obtuse marginal; PDA: posterior descending; PLA: posterolateral; PPV: positive predictive value; RCA: right coronary artery

- **ML model for recognition of coronary artery segment and lesion morphology.**
- **20,612 angiograms of 10,373 patients in China were collected.**

For segment recognition

- **recognition accuracy : 98.4%**
- **recognition sensivity : 85.2 %**

EuroIntervention 2021 Vol. 17 Issue 1 Pages 32-40

Training and validation of a deep learning architecture for the automatic analysis of coronary angiography

Tianming Du[1], PhD; Lihua Xie[2], MSc; Honggang Zhang[1], PhD; Xuqing Liu[1], PhD; Xiaofei Wang[3], MSE; Donghao Chen[3], MSE; Yang Xu[3], BSE; Zhongwei Sun[2], MSc; Wenhui Zhou[3], PhD; Lei Song[2], MD; Changdong Guan[2], MSc; Alexandra J. Lansky[4], MD; Bo Xu[2]*, MBBS

Lesion type	Precision rate	Recall rate	F1 score
Stenosis	0.769	0.901	0.829
Total occlusion	0.757	0.871	0.810
Calcification	0.751	0.862	0.802
Thrombus	0.742	0.925	0.823
Dissection	0.790	0.926	0.854

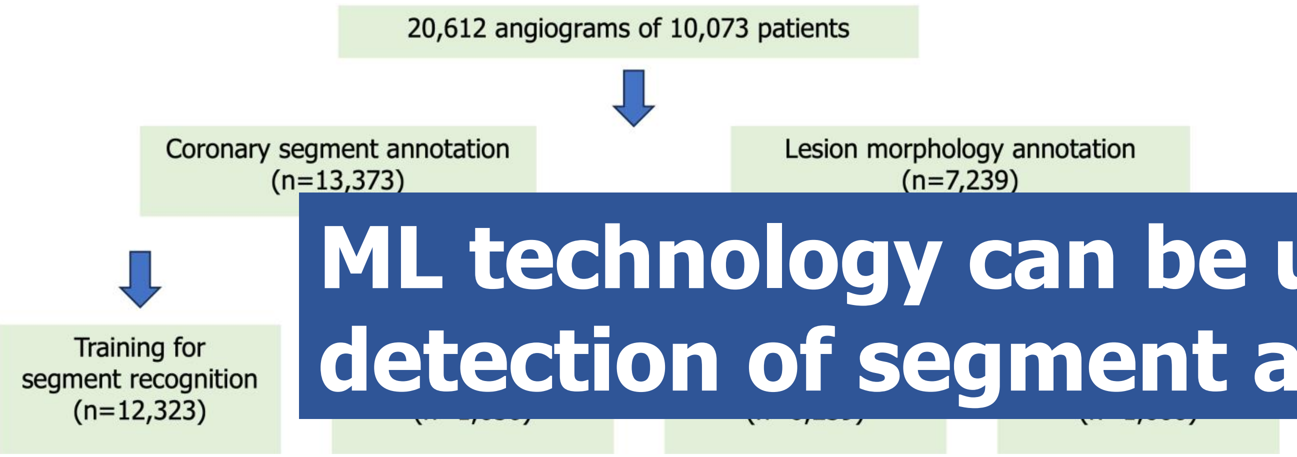

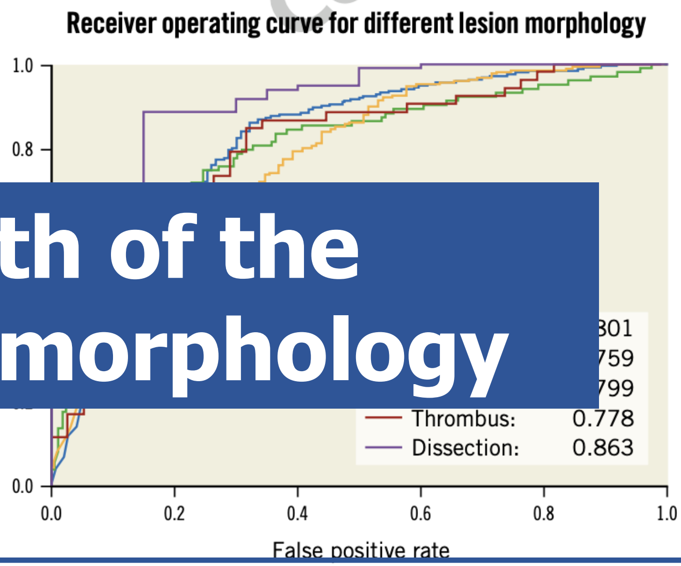

ML technology can be used in both of the detection of segment and lesion morphology

- **ML model for recocnition of coronary artery segment and lesion morphology.**
- **20,612 angiograms of 10,373 patients in China were collected.**

$$\textbf{F1 Score} = \frac{2 \times \text{Precision} \times \text{Recall}}{\text{Precision} + \text{Recall}}$$

F1 score	Interpretation
> 0.9	Very good
0.8 - 0.9	Good
0.5 - 0.8	OK
< 0.5	Not good

For lesion morphology (F1 score)

Stenosis: 0.829
TO: 0.810
Calcification: 0.802
Thrombus : 0.823
Dissection : 0.854

EuroIntervention 2021 Vol. 17 Issue 1 Pages 32-40

Publication of angio-based coronary artery segmentation using AI

Reference	Date	Numbers of angiograms	Algorithm	Results	Limits
Cervantes-Sanchez et al. Appl. Sci. 9, 5507 (2019)	2019	130	Multiscale ANN	ACC: 0.97 DICE: 0.69	High computational demand; difficulties near major vessels
Yang et al. Sci.Rep.9,16897(2019)	2019	3,302	U-Net with Advanced CNN Encoders	F1: 0.94	Limited to single and major coronary arteries; issues with LCA and stenotic regions
Li et al. Neural Information Processing (eds Yang, H. et al.) 185–196 (Springer, 2020)	2020	538	CAU-net	ACC: 0.99 DICE: 0.90	Requires DSA images; suboptimal performance on small vessels
Shi et al. Biology Society (EMBC) 1612–1615 (2020)	2020	4,000	UENet: U-Net generator with multi-scale discriminator	MPA: 0.84	Requires binary images for input
Zhou et al. pre print (2021)	2021	102	U-Net	F1: 0.89	Focuses only on RCA and main coronary arteries; problematic at bifurcations
Iyeret al. Sci.Rep.11,18066(2021)	2021	462	AngioNet: Deeplab v3+ with APN	ACC: 0.98 DICE: 0.86	Tends to overestimate vessel boundaries in severe stenosis; issues with sharp diameter changes
Du et al. EuroIntervention 2021;17:32-40 (2021)	**2021**	**13,373**	**DNN cGAN**	**ACC:0.98**	
Algarni et al. PeerJ Comput. Sci. 8, e993 (2022)	2022	130	Attention-based nested U-net	ACC: 0.97 DICE: 0.92	Difficulties with small vessels and lower-quality images
Menezes et al. Rev. Port. Cardiol. 41, 1011–1021 (2022) Menezes et al. Int. J. Cardiovasc. Imaging 39, 1385–1396(2023)	2022	416	EfficientUNet ++	ACC: 0.99 DICE: 0.95	Struggles with catheter discrimination, poor image quality, and severe stenosis
Roy et al. Comput. Model. Eng. Sci. 136, 241–255 (2023)	2023	28	U-Net	ACC: 0.98	Limited by a small dataset; concerns over broad applicability
Meng et al. Technol. Health Care 31, 2303–2317 (2023)	2023	616	U-Net 3+	DICE: 0.89	
Shen et al. Int. J. Cardiovasc. Imaging 39, 1571–1579 (2023)	2023	70	DBCU-Net: U-Net combining DenseNet and bi- directional ConvLSTM	ACC: 0.99 F1: 0.88	Small dataset size; questions regarding generalizability
Fu et al. Pattern Recognit. 145, 109926 (2024)	2024	217	TV-TRPCA, TSRG	F1: 0.93	Filtering process may reduce precision
Zhang et al. Alex. Eng. J. 87, 201–212 (2024)	2024	1,000	CIDN: U-Net, introducing BAB and MIB	ACC: 0.98 F1: 0.87	

ANN = artificial neural network, ACC accuracy, DICE dice coefficient, MPA mean pixel accuracy, F1 F1 score, TV-TRPCA total variation-tensor robust principal component analysis, TSRG two-stage region growing, BAB bio-inspired attention block, MIB multi-scale interactive block, DSA digital subtraction angiography.

Modified a table from ***Scientific Reports 2024 Vol. 14 Issue 1 Pages 6640***

ARTICLE OPEN

Check for updates

CathAI: fully automated coronary angiography interpretation and stenosis estimation

Robert Avram[1,2], Jeffrey E. Olgin[1,3], Zeeshan Ahmed[4], Louis Verreault-Julien[4], Alvin Wan[3], Joshua Barrios[1], Sean Abreau[1], Derek Wan[5], Joseph E. Gonzalez[5], Jean-Claude Tardif[2], Derek Y. So[4], Krishan Soni[1] and Geoffrey H. Tison[1,3,5,6]✉

- **ML (multiple purpose-built neural networks) model for angiographic coronary stenosis assessment.**
- **10,797 patients; 12,217 angiographic studies, 114,468 videos from UCSF were applied to the model as internal validation.**
- **The model was validated to 464 videos from UOHI cohort.**

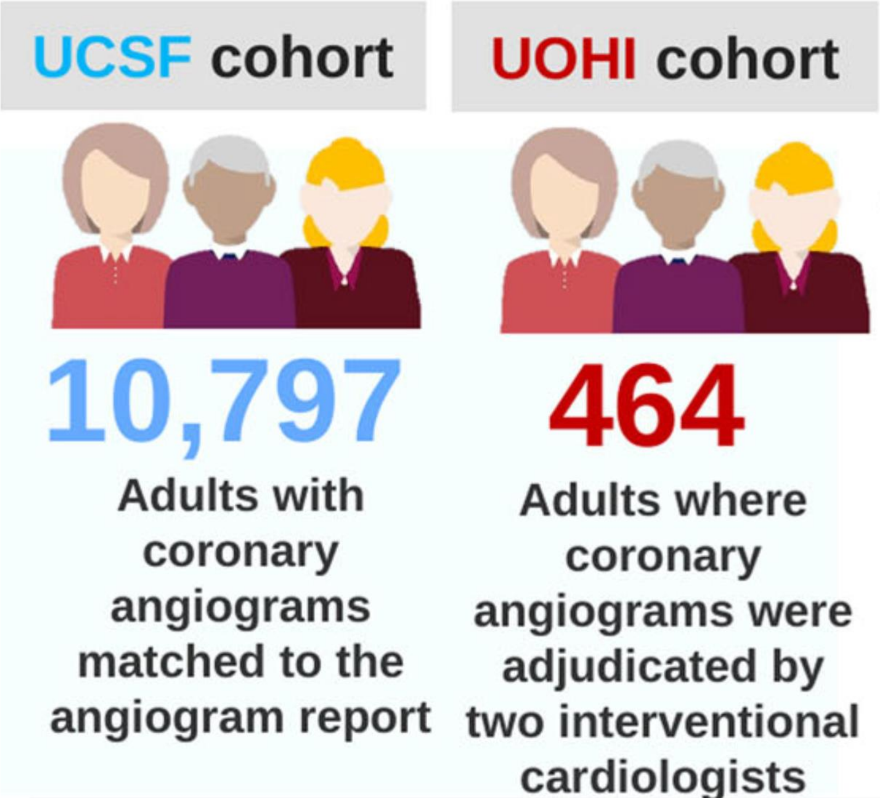

NPJ Digit Med. 2023 Aug 11;6(1):142.

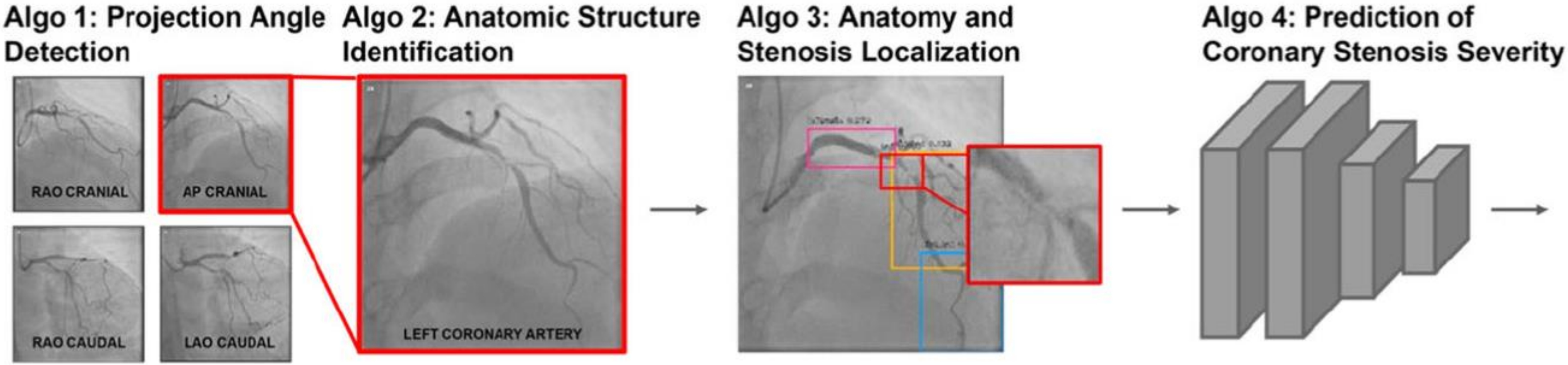

Cohort	Projection Detection F1 Score:	Anatomic Structure Identification PPV* :	Stenosis Localization PPV:	Stenosis Severity Discriminating between severe (≥70%) and non-severe stenosis AUC:
UCSF	0.90	97% & 93%	93.3%	0.862
UOHI	0.81	100% & 100%	84.5%	0.869

ML could increase reproducibility of angiographic coronary stenosis severity assessment.

NPJ Digit Med. 2023 Aug 11;6(1):142.

Publication of angio-based coronary artery stenosis assessment using AI

Reference	Date	Methods	Data	Classes	Resluts
Moon et al. Comput. Methods Programs Biomed. 2020, 198, 105819.	2020	GoogleNet Inception-v3, CBAM, Grad-CAM	452 clips	Stenosis ≥ 50%	AUC = 0.971, accuracy = 0.934
Ovalle-Magallanes et al. Mathematics 2020, 8, 1510.	2020	pre-trained CNN via Transfer Learning, CAM	10,000 artificial images, 250 real images	Stenosis	Accuracy = 0.95, precision = 0.93,
Zhao et al. Comput. Biol. Med. 2021, 136, 104667.	2021	FP-U-Net++, arterial centerline extraction,diameter calculation, arterial stenosis detection	99 patients, 314 images	1–24%, 25–49%, 50–69%, 70–100%	Precision = 0.6998, recall = 0.6840, sensitivity = 0.98, specificity = 0.92, F1 score = 0.95
Antczak et al. MATEC Web Conf. 2018, 210, 04001.	2021	A patch-based CNN for stenosis detection	10,000 artificial images, 250 real images	Stenosis	Accuracy = 90%
Du et al. EuroIntervention 2021, 17, 32–40.	2021	A DNN for the recognition of lesion morphology	10,073 patients, 20,612 images	Stenotic lesion, total occlusion, calcification, thrombus, and dissection	F1 score = 0.829, 0.810, 0.802, 0.823, 0.854
Danilov et al. Sci. Rep. 2021, 11, 7582.	2021	Comparison of state-of-the-art CNN (N = 8)	100 patients, 8325 images	Stenosis ≥ 70%	mAP = 0.94, F1 score = 0.96, prediction speed = 10 fps
Pang et al. Comput. Med. Imaging Graph. 2021, 89, 101900.	2021	Stenosis-DetNet with SFF and SCA	166 sequence, 1494 images	Stenosis	Accuracy = 94.87%, Sensitivity 82.22%
Algarni et al. PeerJ Comput. Sci. 2022, 8, e933.	2022	ASCARIS model	130 images	normal and abnormal	Accuracy = 97%, recall = 95%, specificity = 93%
Liu et al. Appl. Sci. 2023, 13, 2975.	2023	AI-QCA	3275 patients, 13,222 images	0–100%	Precision = 0.897, recall = 0.879
Cong et al. Front. Cardiovasc. Med. 2023, 10, 944135.	2023	Inception-v3 and LSTM, redundancy training, and Inception-V3, FPN	230 patients, 14,434 images	<25%, 25–99%, CTO	Accuracy = 0.85, recall = 0.96, AUC = 0.86
Ling et al. J. Cardiovasc. Transl. Res. 2023, 16, 896–904.	2023	DLCAG diagnose system	949 patients, 2980 images	Stenosis	mAP = 86.3%
Avram et al. npj Digital Medicine , 2023, 6:142	2023	fully-trained CathAI algorithms	**10,797 patients,** 114,468 images for internal validation 464 patients, 464 images for external validation	Stenosis ≥ 70%	**AUC for internal validation : 0.862 AUC for external validation 0.869**

Modified a table from ***Diagnostics 2023 Vol. 13 Issue 18 Pages 3011***

Angio-imaging vs. CTCA

Angiography

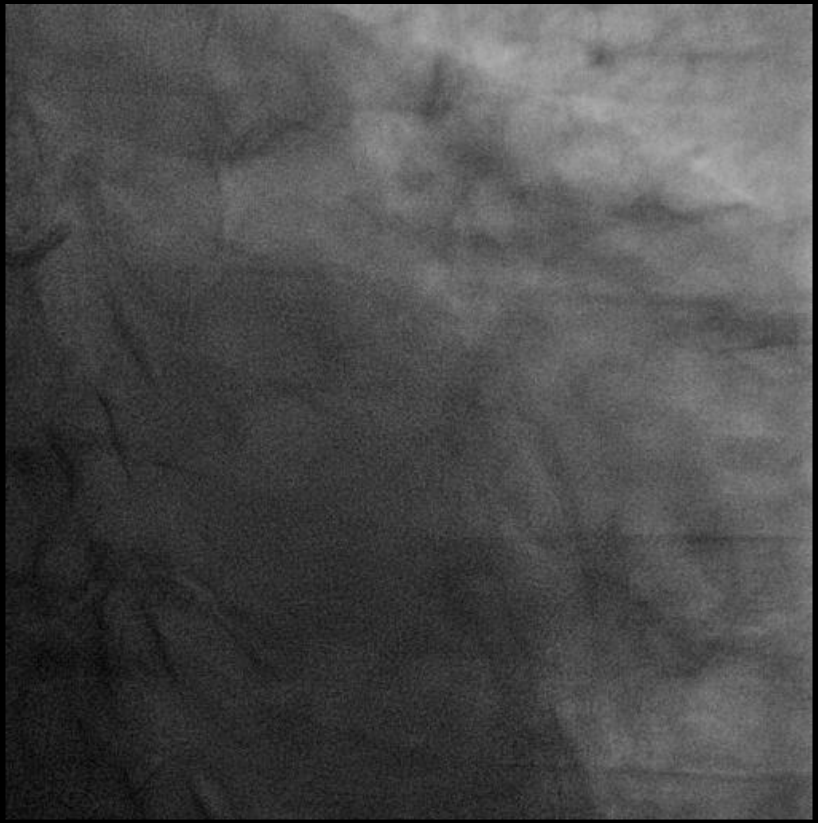

Murray law-based QFR

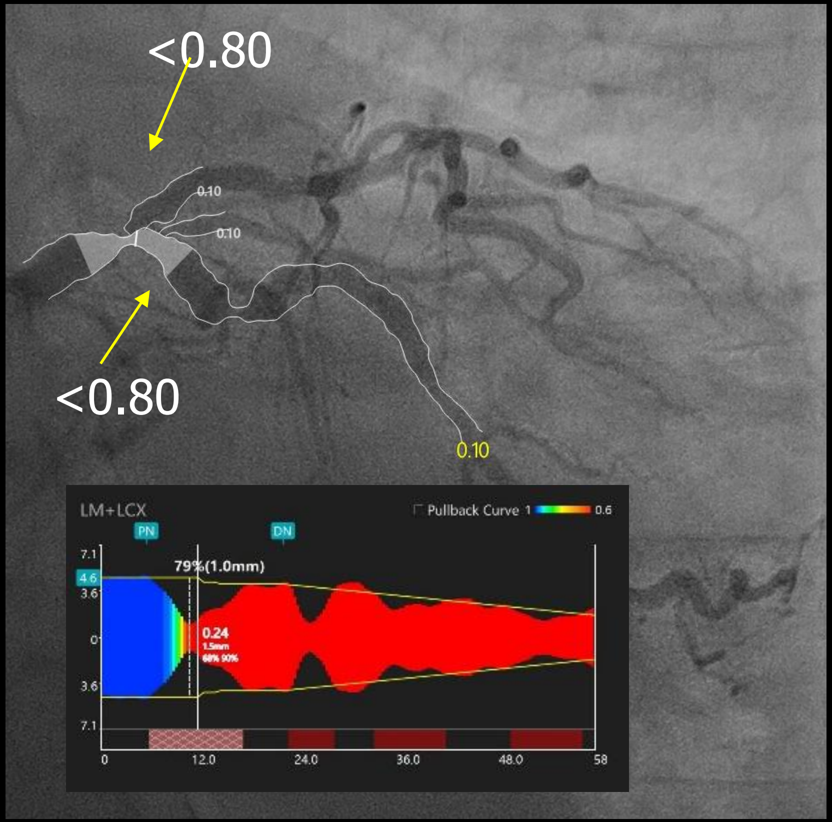

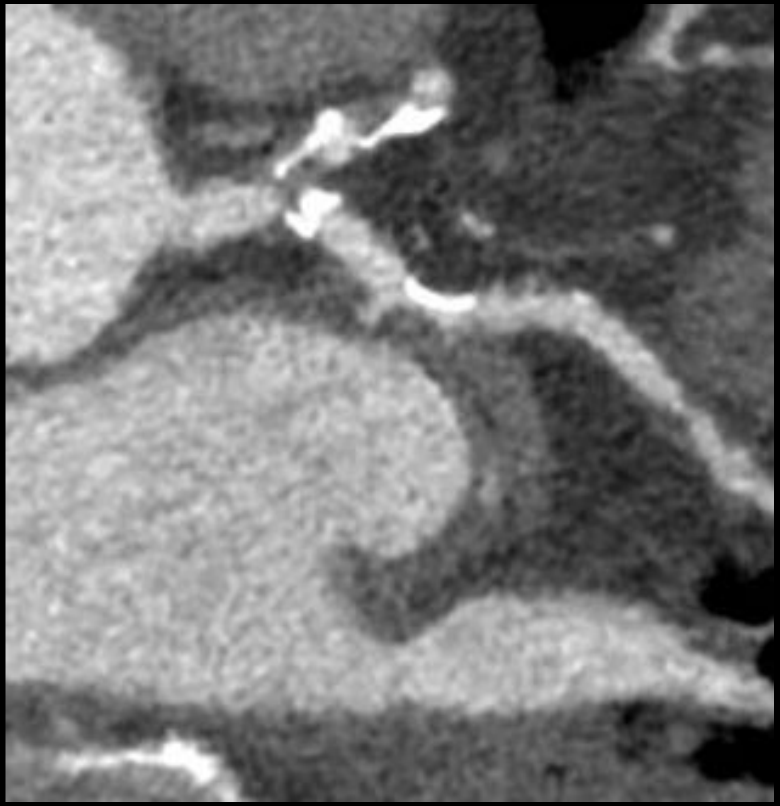

Commercially available angio-based FFR softwares

	μQFR	QFR	FFR$_{\text{angio}}$	vFFR	caFFR	angioFFR	AutocathFFR
Company	Pulse Medical	Medis	CathWorks	Pie Medical	RainMed	Siemens	Medhub Ltd.
Estimated reference	FFR	FFR	FFR	FFR	FFR	FFR	FFR
Required angio projections	1 projection	2 projections (>25° apart)	3 projections (>30° apart)	2 projections	2 projections (>30° apart)	2 projections (>30° apart)	2 projections
Required pressure data	No	No	No	Need	Need	No	No
Side branches	+	-	+	-	-	+	NA
Computation method	Kirkeeide	Lance Gould equation	Electric circuit model	Simplified Navier–Stokes	Simplified Navier–Stokes	AI based	AI based
Studies	Tu S, et al.	FAVOR pilot FAVOR II China FAVOR II EJ FAVOR III	FAST-FFR	FAST FAST II	FLASH-FFR FLASH II	Omori, Matsuo, et al.	Presented at CRT2022
C-statistics	0.97	0.92-0.96	0.94	0.93	0.98	0.90	0.93
Time to computation	67 sec	4.4 min	2.7 min	NA	4.5 min	NA	45 sec

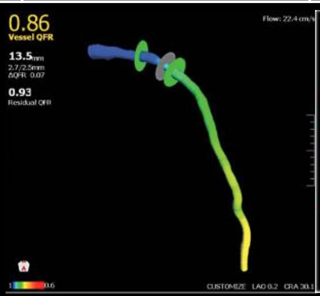

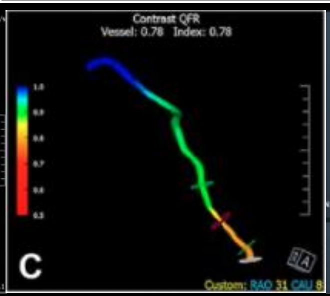

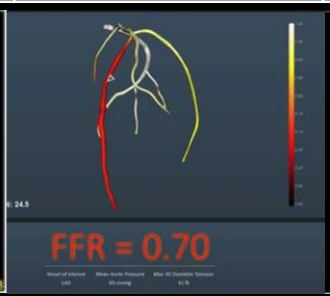

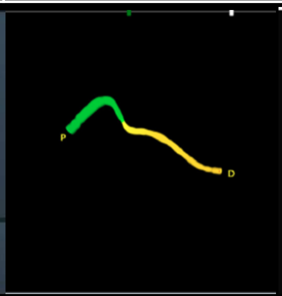
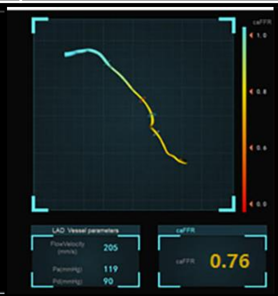

Commercially available angio-based FFR software's

	µQFR 2D and 3D	QFR	FFR_{angio}	vFFR	caFFR	angioFFR	AutocathFFR
Company	**Pulse Medical**	**Medis**	CathWorks	**Pie Medical**	**RainMed**	Siemens	Medhub Ltd.
Estimated reference	**FFR**	**FFR**	FFR	**FFR**	**FFR**	FFR	FFR
Required angio projections	**1 projection Or 2 projections**	**2 projections (>25° apart)**	3 projections (>30° apart)	**2 projections**	**2 projections (>30° apart)**	2 projections (>30° apart)	2 projections
Required pressure data	**No**	**No**	No	**Need**	**Need**	No	No
Side branches	**+**	**-**	+	**-**	**-**	+	NA
Computation method	**Kirkeeide**	**Lance Gould equation**	Electric circuit model	**Simplified Navier–Stokes**	**Simplified Navier–Stokes**	AI based	AI based
Studies	**Tu S, et al.**	**FAVOR pilot FAVOR II China FAVOR II EJ FAVOR III**	FAST-FFR	**FAST FAST II**	**FLASH-FFR FLASH II**	Omori, Matsuo, et al.	Presented at CRT2022
C-statistics	**0.97**	**0.92-0.96**	0.94	**0.93**	**0.98**	0.90	0.93
Time to computation	**67 sec**	**4.4 min**	2.7 min	**NA**	**4.5 min**	NA	45 sec

Diagnostic performance of each software against wire-FFR ≤0.80

A. ROC curves for each angiography derived FFR to detect an FFR of ≤0.80

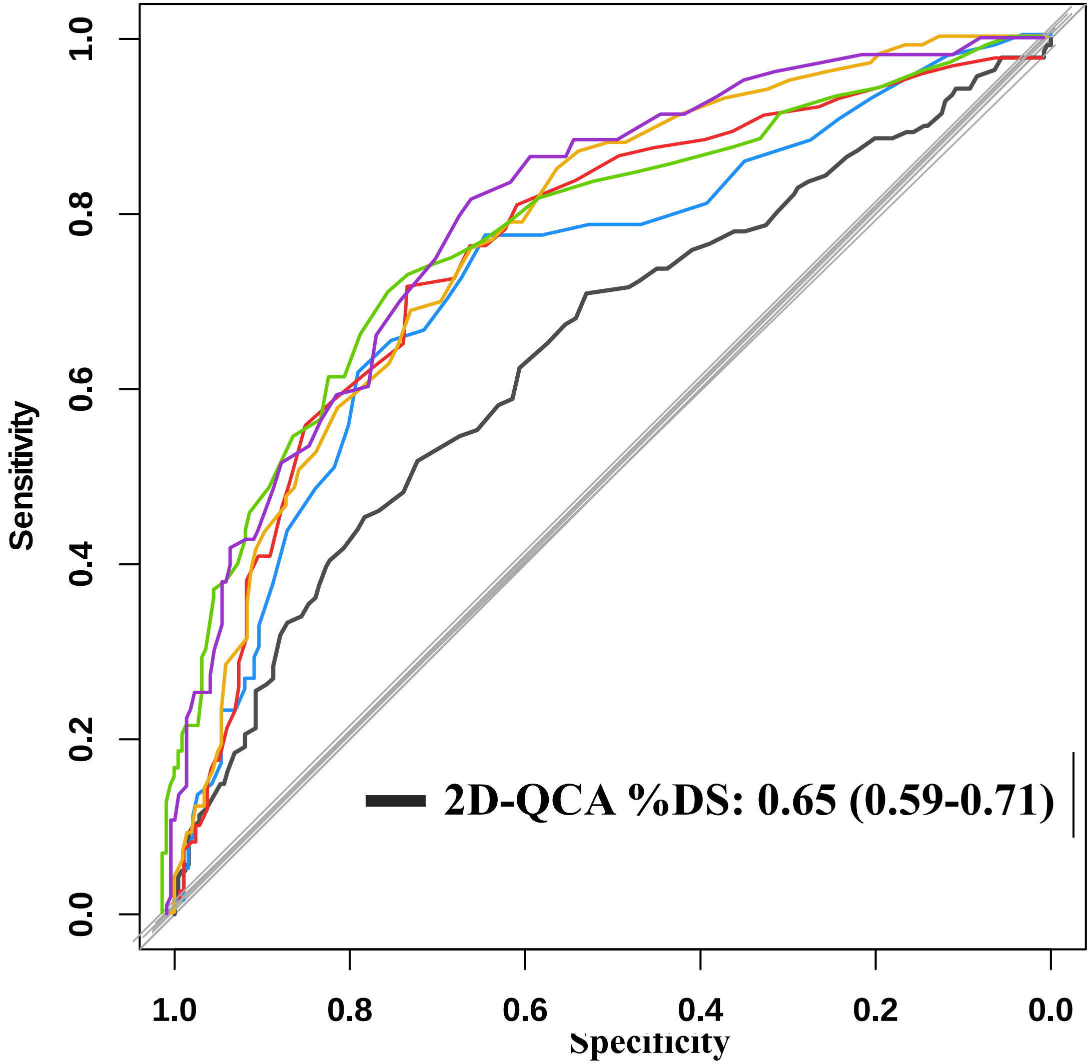

Threshold of A, B, C, D, E, and 2D-QCA %DS was 0.82, 0.81, 0.82, 0.81, 0.80, and 47%

Software	AUC	boot-strapped 95% CI
Software A	0.753	0.698-0.801
Software B	0.743	0.690-0.795
Software C	0.735	0.682-0.783
Software D	0.732	0.676-0.785
Software E	0.730	0.675-0.784

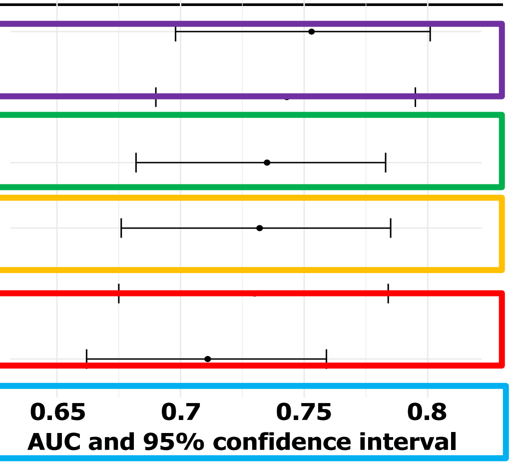

The AUC of five angiography-derived FFR software/methods for predicting a wire-FFR ≤0.80 was comparable, with a higher AUC compared to 2D-QCA, however it didn’t reach the diagnostic accuracy (AUC≥0.9) reported in validation studies from the various vendors.

Ninomiya et al. JACC int 2023

Predictors of false positive and false negative

✔ **Binary logistic regression analysis showed the predictors of false positives and false negative.**

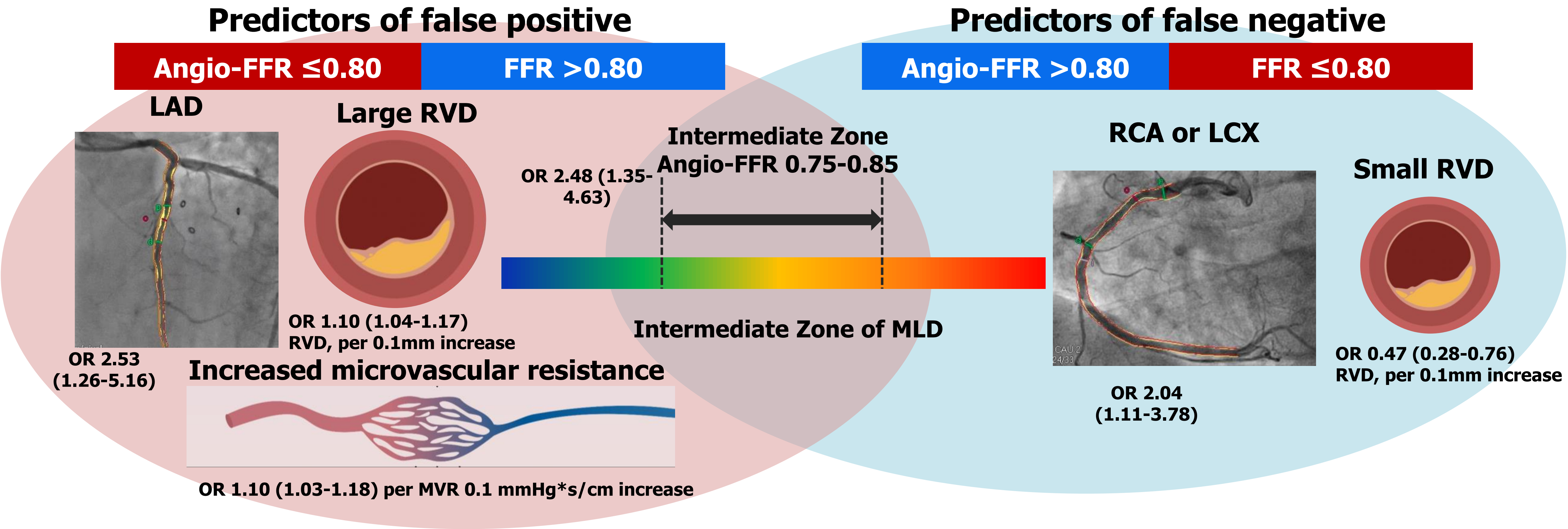

Severity of lesion stenosis, lesion location, microvascular resistance, and intermediate zone of angiography-derived FFR potentially reduce the diagnostic accuracy.

Ninomiya et al. JACC int 2023

Ongoing Clinical Trials to investigate clinical impact of angio-based FFR guidance

Investigation Topic	Type of Trial	Patient No. & Country
FAVOR III Europe Japan Trial QFR vs. FFR in patients with CCS + intermediate stenosis & ACS + intermediate stenosis in non-culprit vessel	Multi-center RCT	2000 patients **NCT03729739**
PIONEER IV Trial QFR guidance vs. Usual care guidance in all-comer patients referred to angiography with at lease 1 significant lesion (DS≥50%) for PCI	Multi-center RCT	2540 patients Europe **NCT04923191**
AQVA QFR-based-Virtual PCI vs. Angio-guided PCI	2 centers, RCT	300 patients Italy **NCT04664140**
MULTIVESSEL TALENT Trial QFR guided Revascularization in multivessel CAD.	Multi-center RCT of Supraflex vs Synergy in multivessel CAD	1550 Patients Europe **NCT04390672**
FAST III **vFFR** guided versus FFR guided coronary revascularization in intermediate coronary lesions	Multi-center RCT	2228 patients Europe **NCT04931771**

Pullback pressure gradients index - PPG_{index}

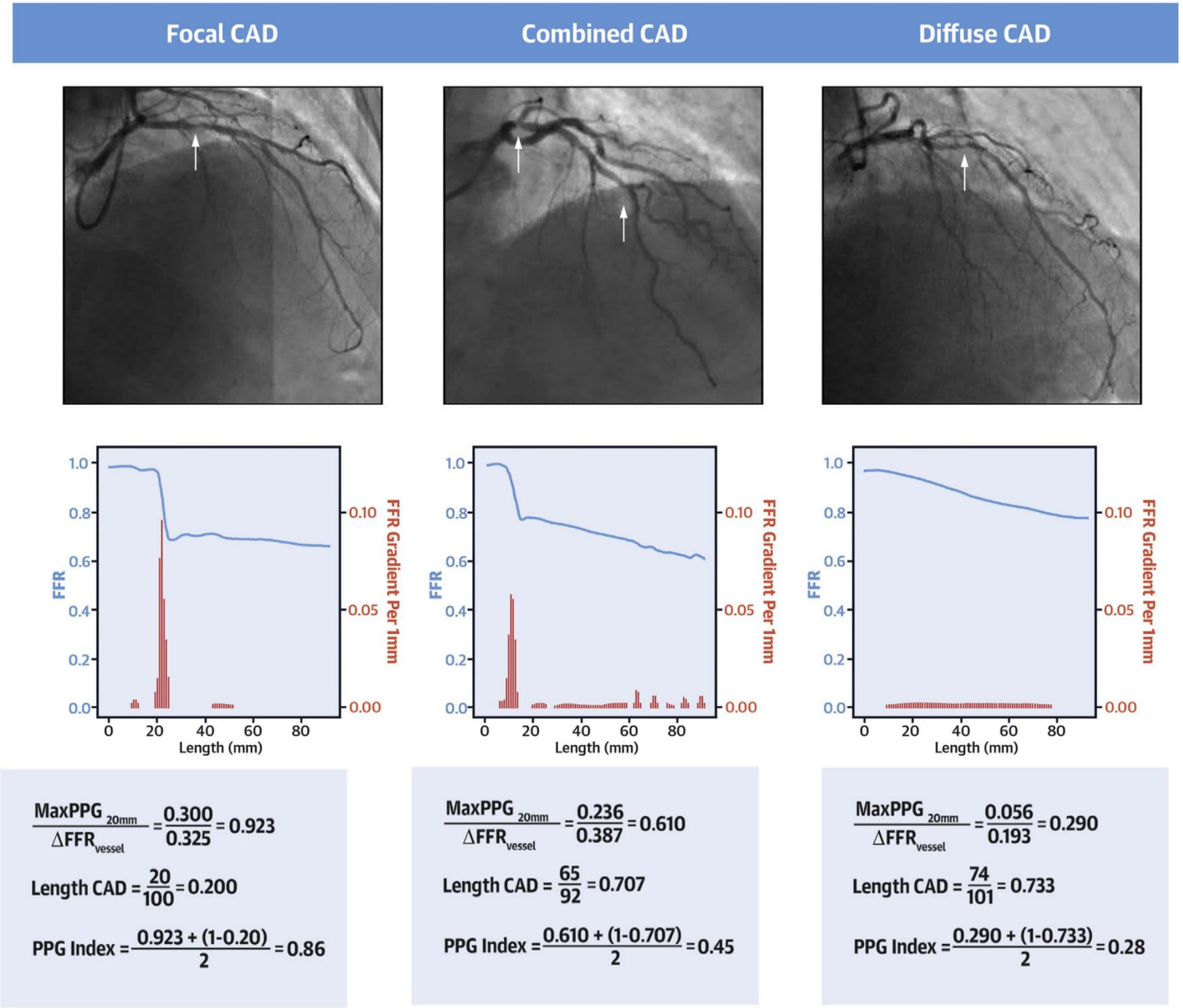

- **Motorized pullback (1mm/sec) and continuous hyperaemia induction**
- **Granularity (Resolution)= 1 mm**
- **FFR ≥0.95 no functional disease**
- **No co-registration**

Pullback Pressure Gradients Index Formula: {$MaxPPG_{20mm}/\Delta FFR_{vessel}$+ (1-Length with Functional Disease(mm)/Total Vessel Length(mm))}/2

Collet C et al. J Am Coll Cardiol. 2019;74(14):1772–84

Disease Patterns According to QFR PPG index and dQFR/ds

Ollscoil na Gaillimhe
University of Galway

CORRIB CORE LAB:

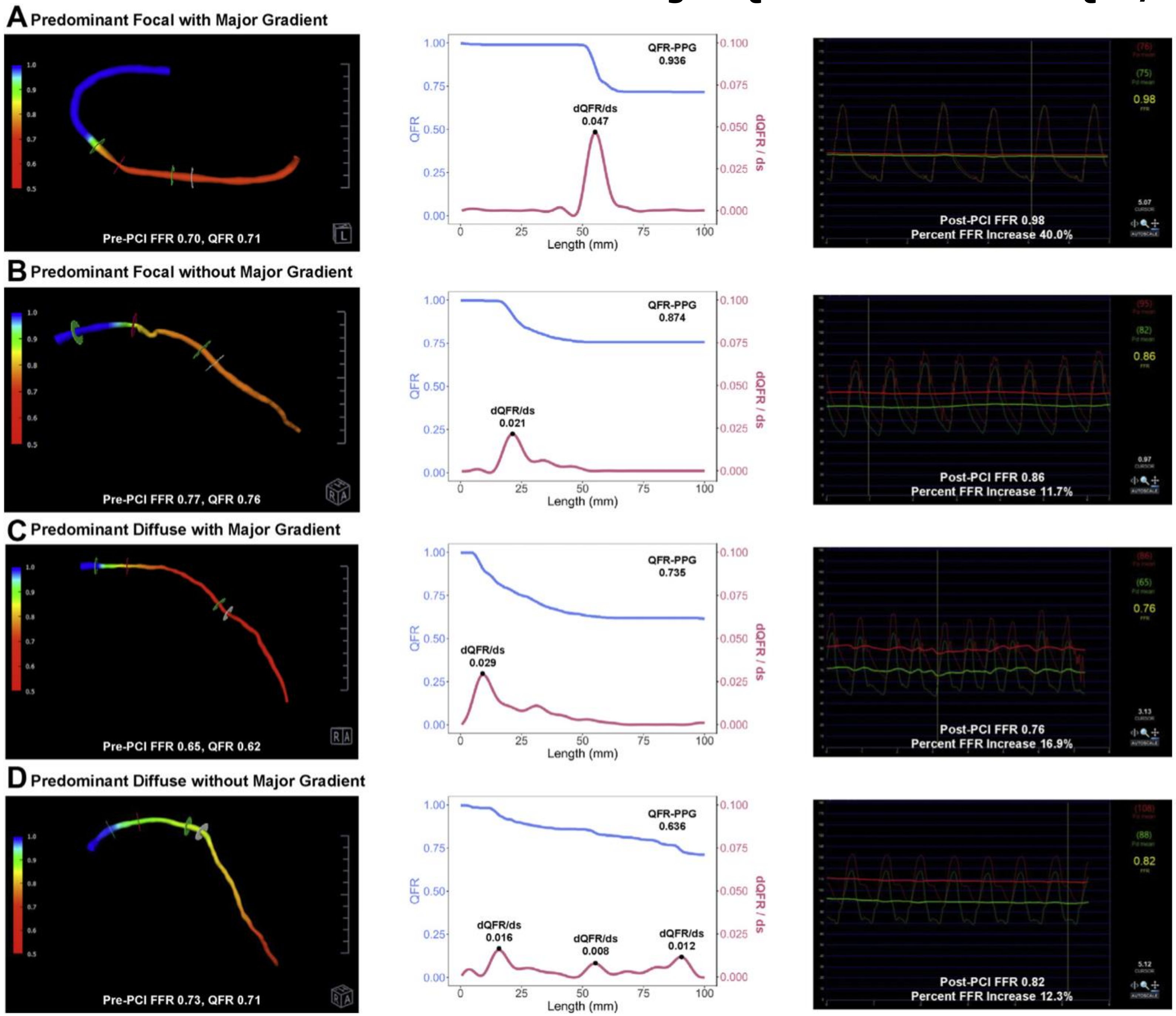

Shin D et al. JACC Cardiovasc Interv. 2021 Aug 23;14(16):1771-1785

Physiological Diffuseness assessment on Angio in ASET Japan trial

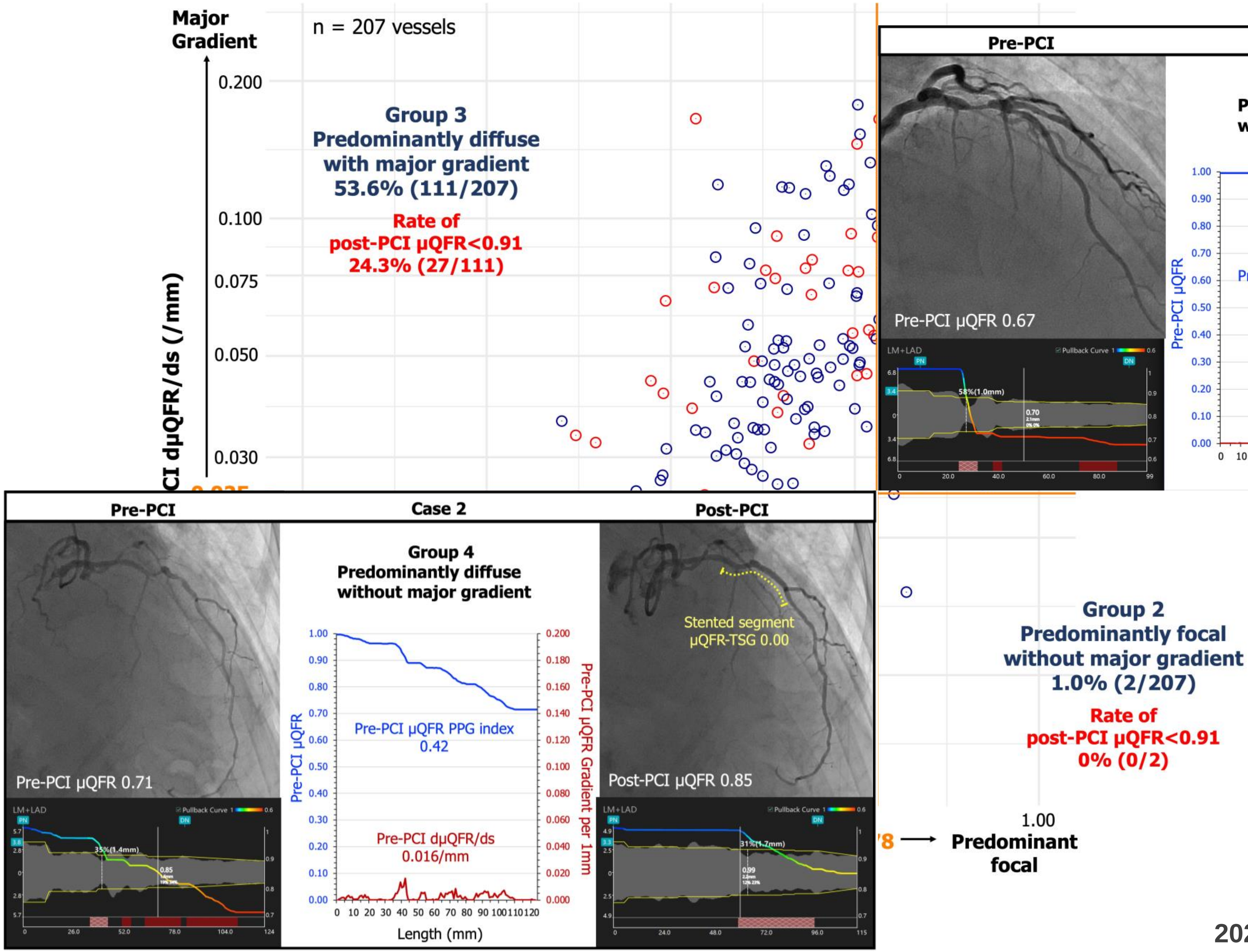

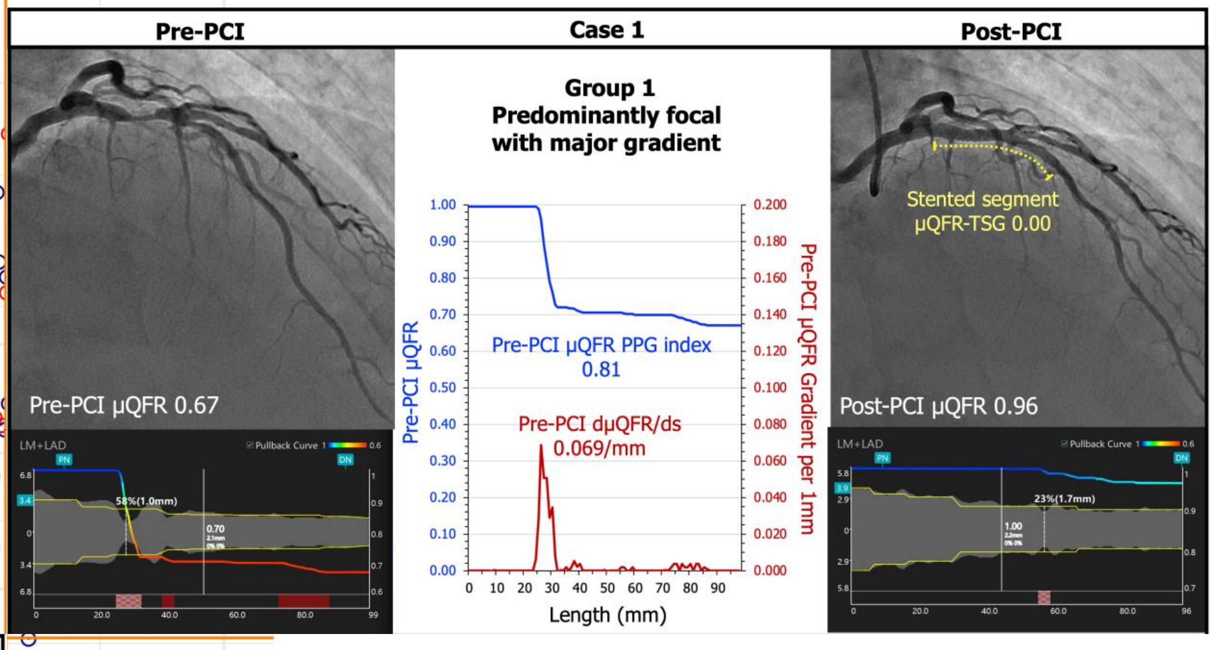

- **Red dots show vessels with post-PCI μQFR <0.91, and blue dots show those with ≥0.91.**
- **Low pre-PCI μQFR value** and **low μQFR PPG index (diffuse disease)** were significantly associated with **increased risk of post-PCI μQFR <0.91**.

Kotoku et al. Eurointervention 2023
2023;19-online publish-ahead-of-print November 2023

Index of Microvascular Resistance

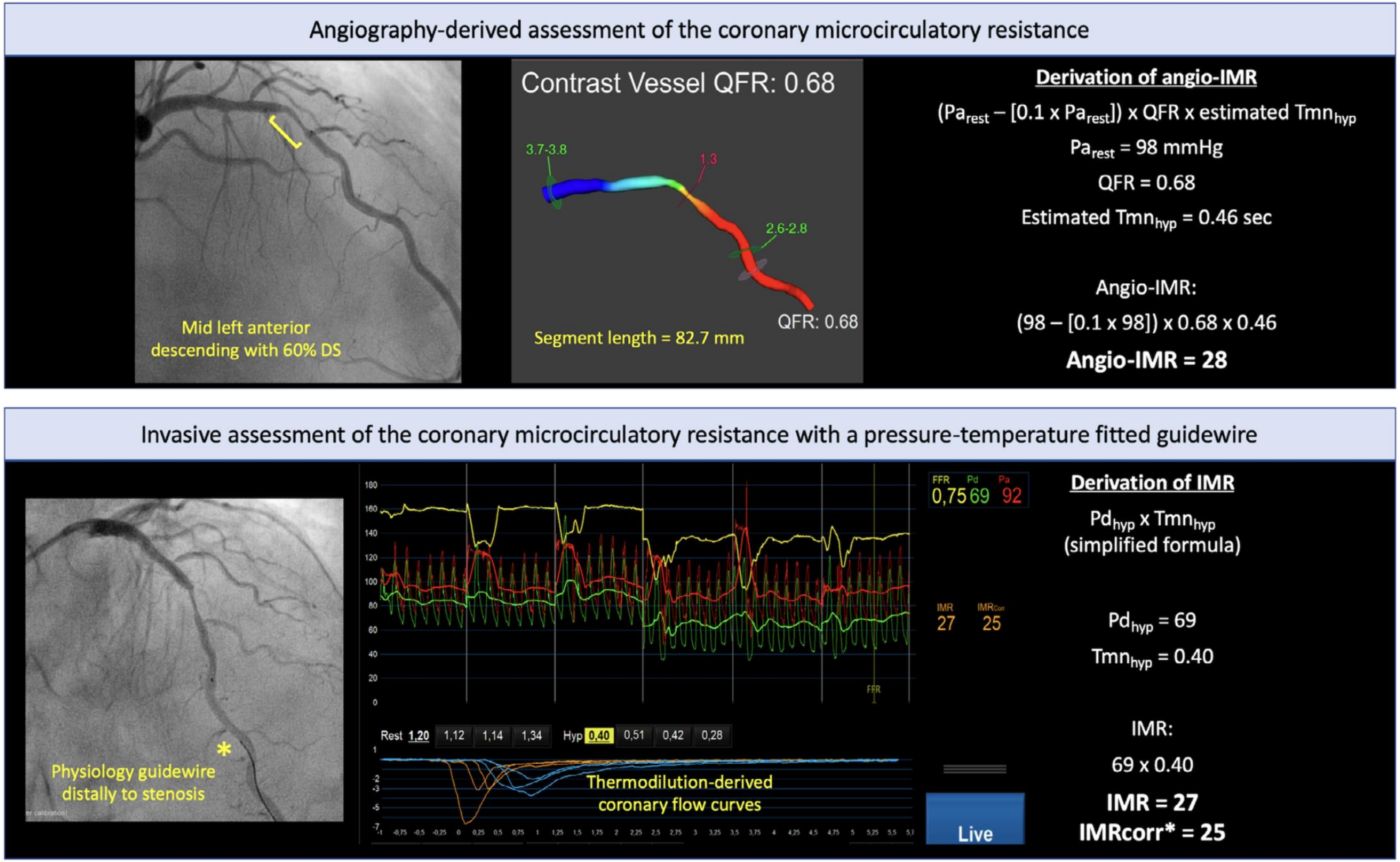

Hernan Mejia-Renteria, Javier Escaned et al. 2021. Catheter Cardiovascular Interventions

Pathophysiological phenotypes in ongoing studies pre and post PCI (n=1004 Vessels)

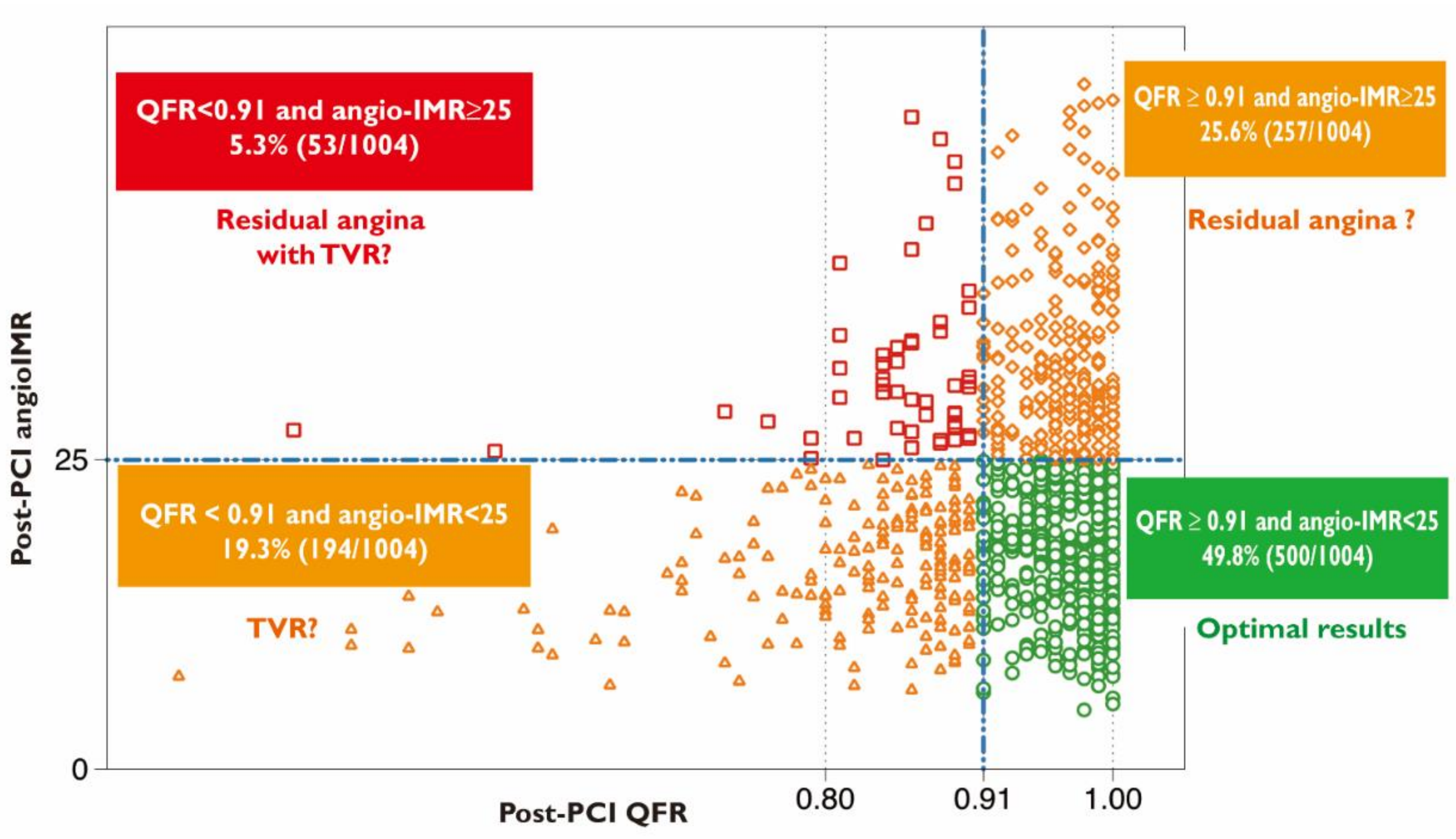

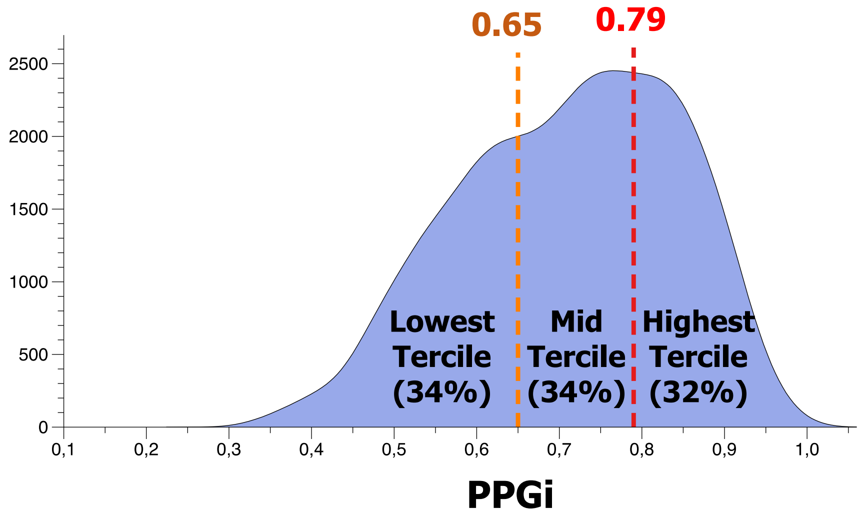

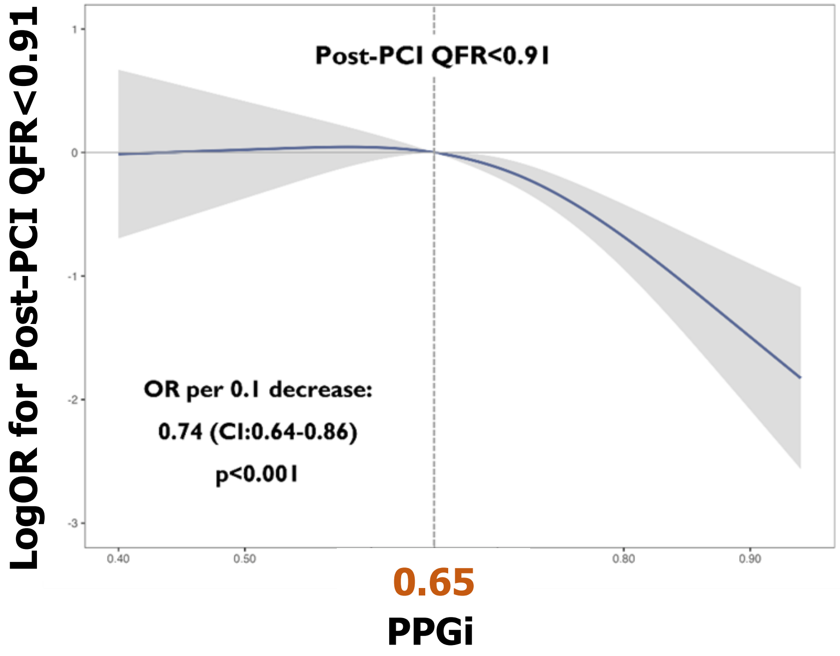

CTCA

MIP

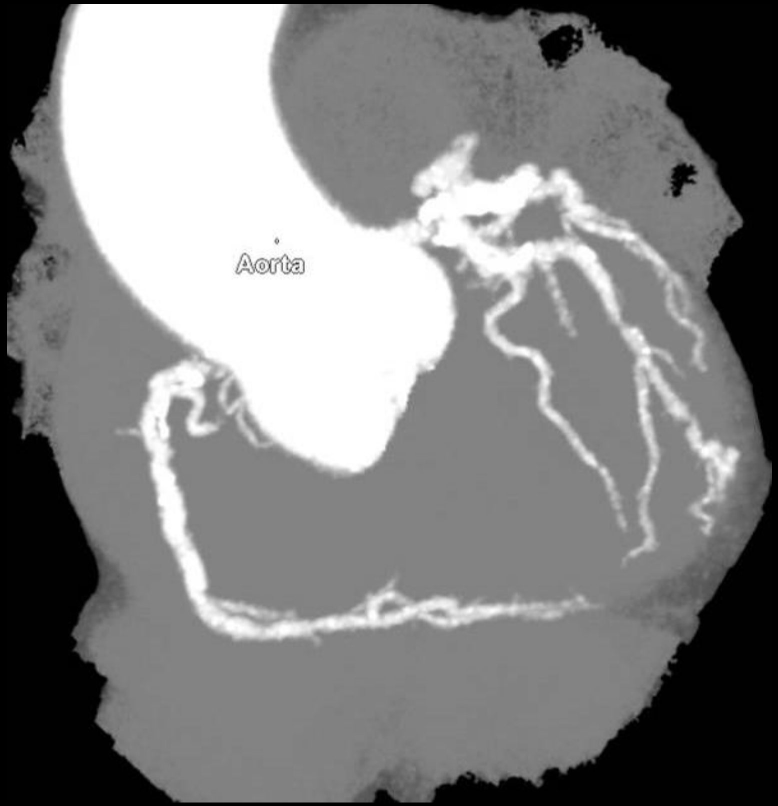

MPR

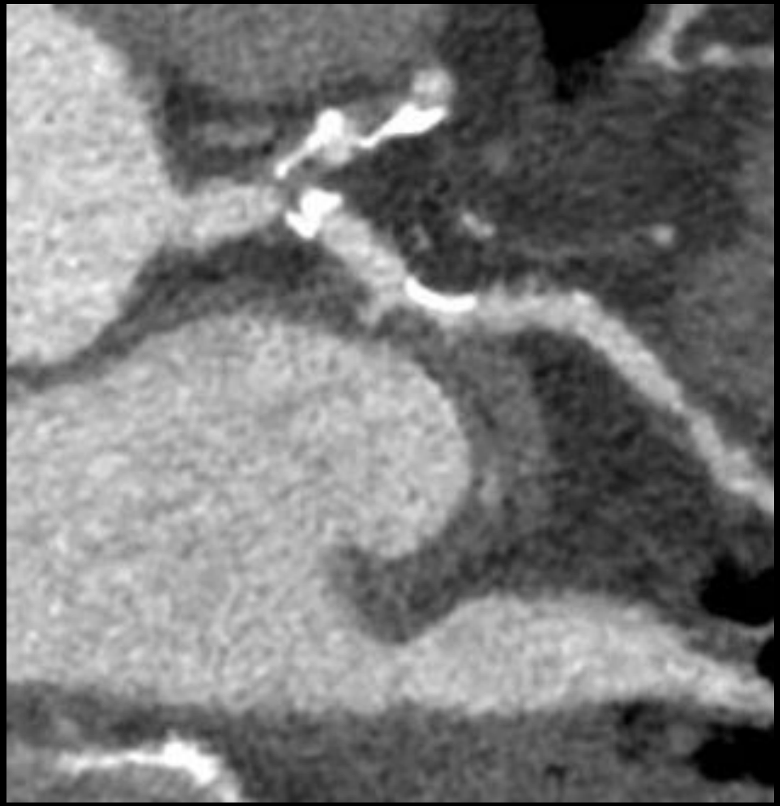

FFRCT

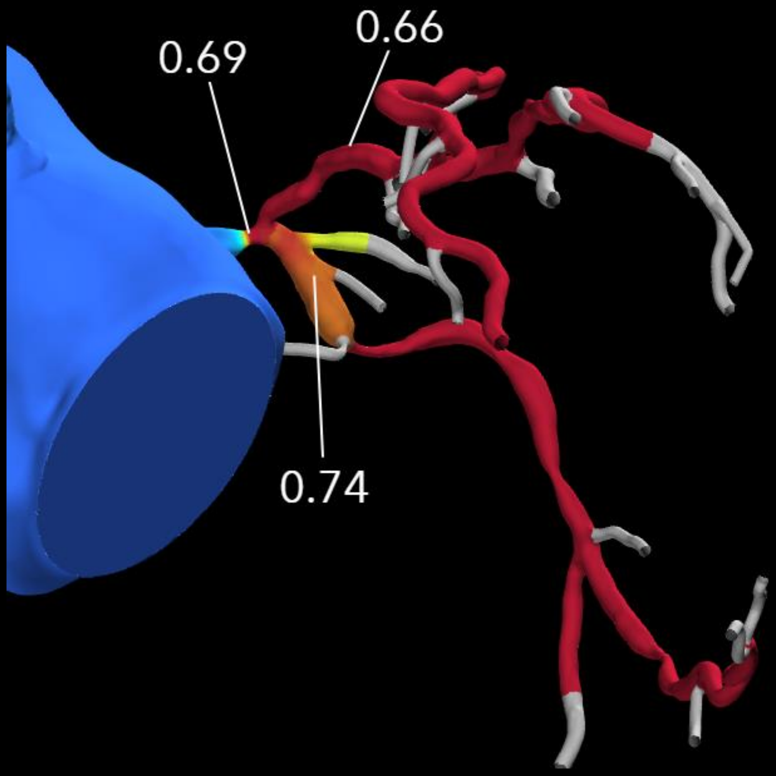

An excellent correlation for plaque volume quantification between CCTA and IVUS (r = 0.98)

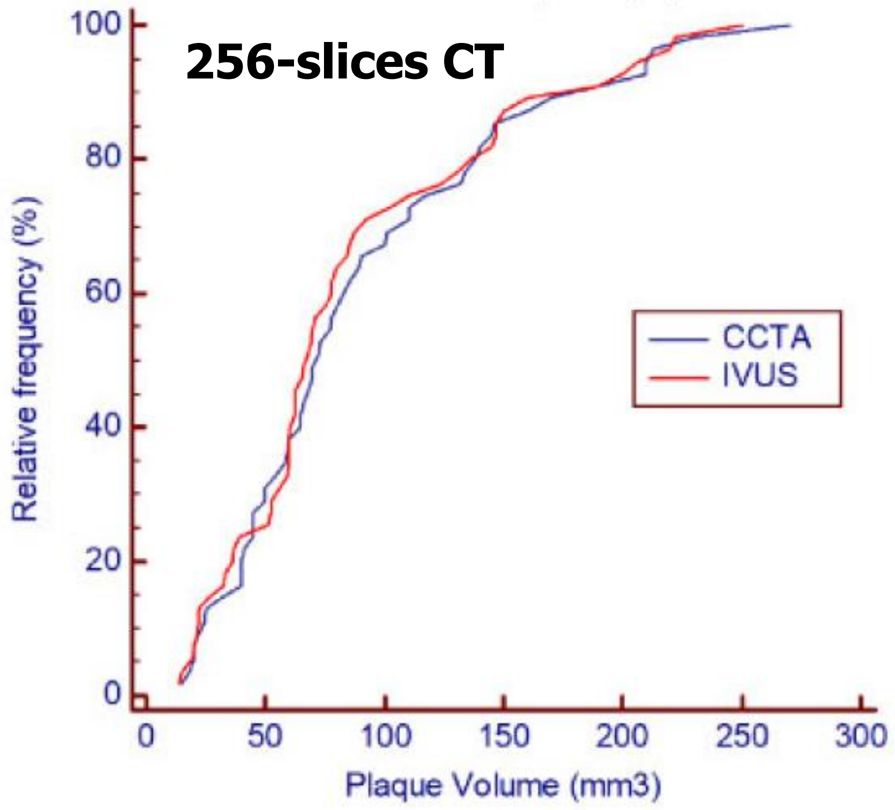

Conte, Mushtaq and Andreini et al.Eur Heart J Cardiovasc Imaging. 2020 Feb 1;21(2):191-201

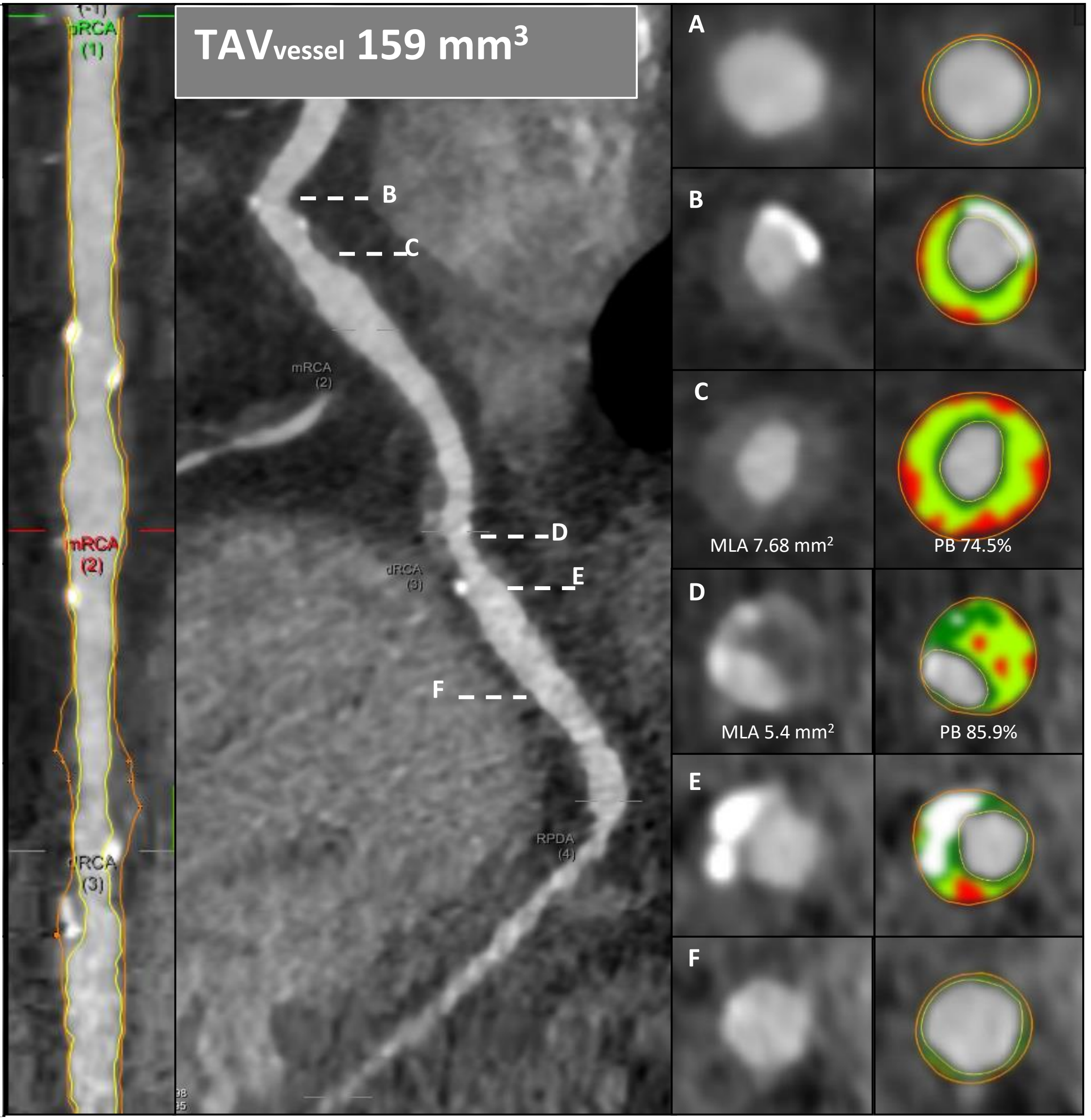

Plaque Composition detected by CTA

Dense calcium **Fibrous** **Fibro-fatty** **Low-attenuation**

Deep Learning-enabled Coronary CT Angiography for Plaque and Stenosis Quantification and Cardiac Risk Prediction: An International Multicentre Study

Segment coronary plaque assessment by a novel deep learning convolutional neural network

- Training cohorts: 921 patients (5045 lesions)
- Independent test set: external validation cohort of 175 patients (1081 lesions) and 50 patients (84 lesions) assessed by IVUS
- Excellent agreement between **deep learning vs. expert readers** for **calcified plaque volume (ICC 0.964)** and **%DS (ICC 0.879)**
- Excellent agreement between **deep learning vs. IVUS** for **total plaque volume (ICC 0.949)** and **MLA (ICC 0.904)**
- A **deep learning-based total plaque volume ≥238.5mm³** was associated with an **increased risk of MI (HR 5.36, 95% CI 1.70–16.86; p=0.0042)**.

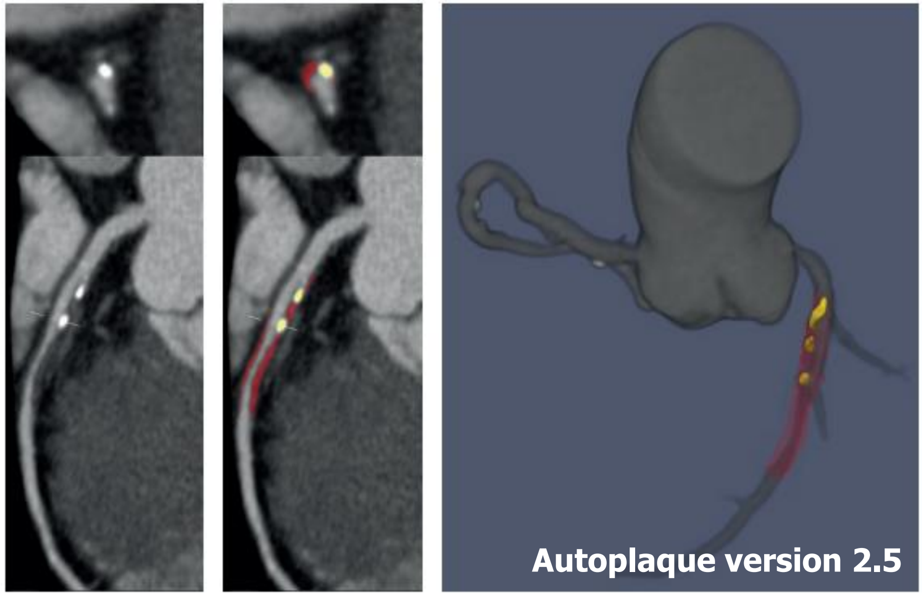

Total plaque volume measured by deep learning vs. IVUS

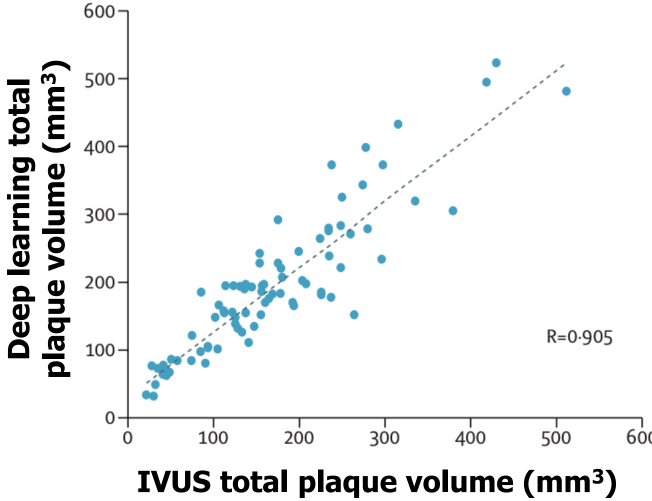

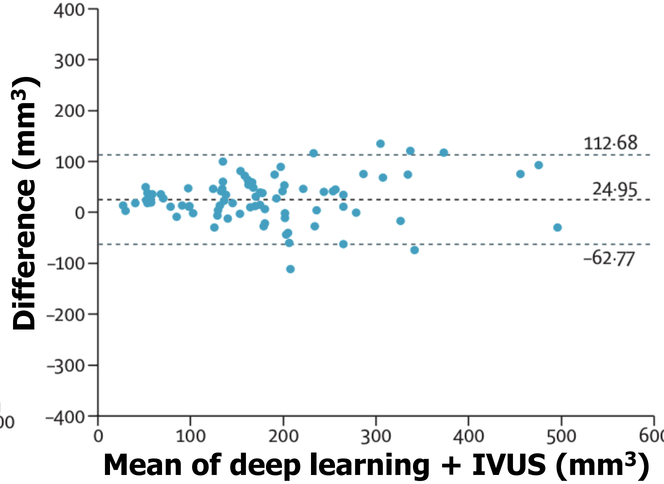

	ICC (95% CI)	Spearman correlation
Total plaque volume	0.964 (0.960–0.967)	0.922
Noncalcified plaque volume	0.938 (0.932–0.944)	0.906
Calcified plaque volume	0.938 (0.932–0.944)	0.904
Low-attenuation plaque volume	0.810 (0.786–0.831)	0.798
Diameter stenosis	0.879 (0.863–0.895)	0.847

Lin A et al. Lancet Digit Health 2022 4:e256-65.

Commercialy availabe software for quantitative plaque assessment

	SurePlaque	QAngio	Autoplaque	vascuCAP	Cleerly CORONARY	HeartFlow plaque Analysis	Syngo.via Frontier Coronary Plaque Analysis 5.0
vender	Canon Medical Systems, Japan	Medis Medical Imaging Systems, The Netherlands	Cedars-Sinai Medical Center, Los Angeles, CA	Elucid Bioimaging, Wenham, MA	Cleerly Healthcare, New York, NY	HeartFlow, Mountain View, CA	Siemens Healthineers Erlangen, Germany
FDA status	510k 2004	510k 2006	510k 2012	510k 2017	510k 2019	510k 2022	**Research only**
Method	Computer assisted, semi- automated.	Computer assisted, semi- automated.	**AI enabled,** Computer assisted, semi- automated.	**AI enabled,** Computer assisted, semi- automated.	**AI-enabled,** fully automated service.	**AI enabled,** fully automated.	Computer assisted, semi-automated.
Ouptuts	**Stenosis**, Plaque Volume, Vessel Volume, Plaque characteristics	**Stenosis,** Plaque Volume, Vessel Volume, Remodeling Index, Plaque characteristics	**Stenosis,** Plaque Volume, composition, and burden, Vessel Volume, Remodeling Index, Contrast density drop, Plaque characteristics	**Stenosis**, Plaque Volume, Vessel Volume, Remodeling Index, Plaque characteristics	**Stenosis**, Plaque Volume, Vessel Volume, Remodeling Index, Plaque characteristics	**Stenosis**, Plaque Volume, Vessel Volume, Remodeling Index, Plaque characteristics	**Stenosis**, Plaque Volume, Vessel Volume, Remodeling Index, Plaque characteristics
Plaque Characteristics and Thresholds	Low density non calcified (-100 to 49 HU) Non-calcified (50–149 HU) Calcified (150–1300 HU)	Necrotic core (-30 to 30HU) Fibrofatty (31–130 HU) Fibrous (131–350 HU) Dense calcium (351–2048 HU)	Non-calcified *, Calcified * Low density non calcified (<30 HU) Necrotic core, fibrous fatty, fibrous and dense calcium as per QAngio thresholds * Automatically adjusted based on lumen attenuation	Lipid rich necrotic core (<45 HU) Matrix (45–250 HU) Calcified plaque (250 HU)	Low density noncalcified (<30 HU) Noncalcified (<350HU) Calcified (≧350 HU)	low-attenuation plaque <30 HU; calcified plaque derived with adaptive thresholding based on lumen contrast; and non-calcified plaque >30 HU and < calcified plaque threshold	Lipid rich (30 to 30 HU) Fibrotic (32–350 HU) Calcified (>350 HU)

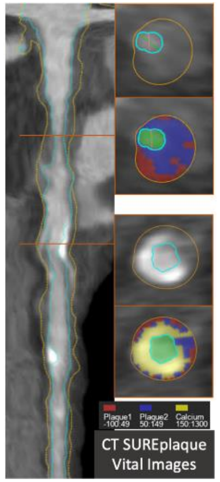

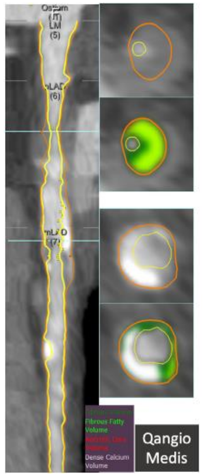

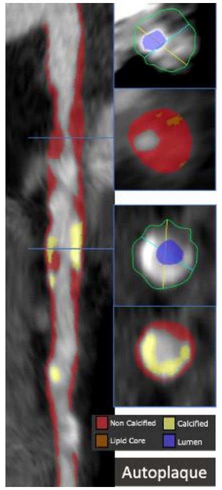

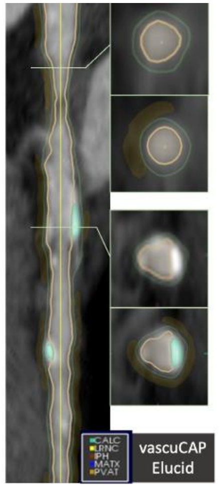

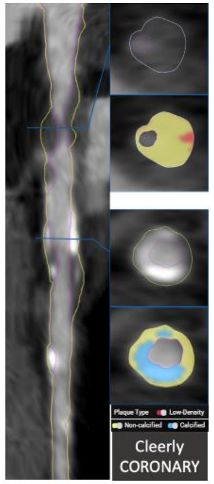

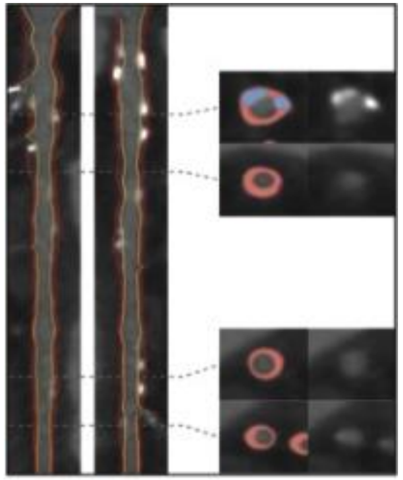

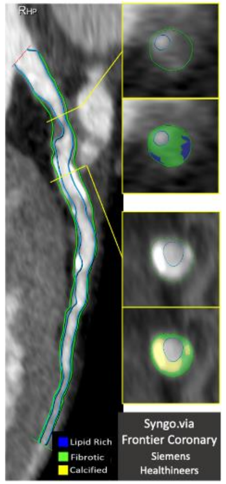

Modified a table from ***Michelle C Williams, et al. J Cardiovasc Comput Tomogr. 2022 ;16(2):124-137. JACC Cardiovasc Imaging. 2024 Feb;17(2):165-175.***

Full-order and on-site CT-derived FFR

	HeartFlow FFR_{CT}	Siemens cFFR		Pulse CT-QFR	Canon CT-FFR	DEEPVESSEL FFR
		Computational Fluid Dynamics-based	Machine Learning-based			
Computation of flow Computational Fluid Dynamics (CFD) Simulation of Coronary Flow	Full 3D CFD modelling by parallel supercomputer	Reduced order CFD modelling by standard desktop computer				
	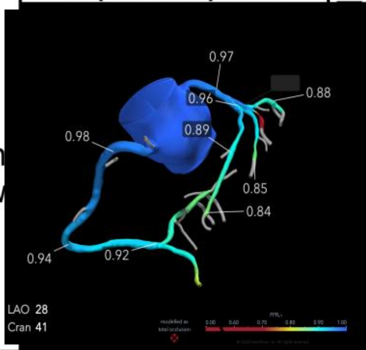	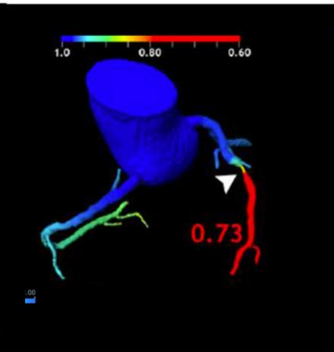		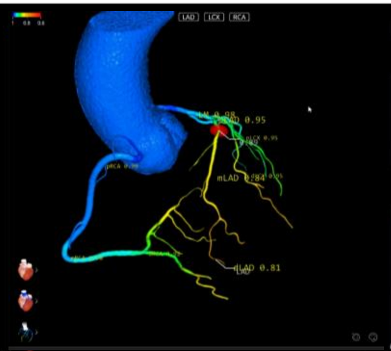	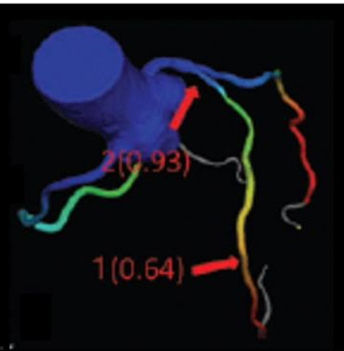	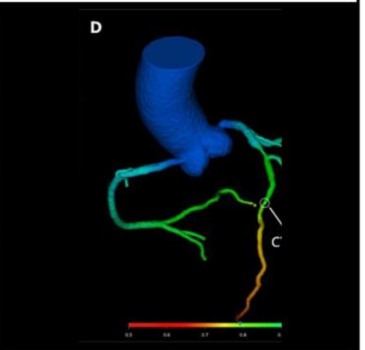
Physiological Model Boundary Conditions Microvascular Resistance	Resting coronary flow(Q) by allometric scaling laws: **Q ∝ myocardial mass** Distribution of coronary flow over 3D model by Murray's law: **Q ∝ d^3** (d: vessel diameter) Patient-specific microvascular resistance (R): **R ∝ d^{-3}** Simulation of hyperemic state by reducing the microvascular resistance			**Q** ~ $V^{\frac{3}{4}}$(V: reference arterial volume) Conversion resting flow to virtual hyperemic flow (HFV): **HFV=0.10+1.55 · RFV -0.93 · RFV^2** (RFV: resting flow velocity)	Coronary flow: •Δ cross-sectional vessel area using 4 diastole phases Microvascular resistance: •minimized during diastole •constant resistance s.t. coronary pressure ∝ flow	Via a professional software which using the CCTA imaging as input and automatically calculate the FFR values of the entire vascular tree based on the deep learning algorithm.
Analysis Time	Full-order model within **4 hours** of data transfer	**30 to 60 min**		**17 min**	**39.4±8.6 min**	**120 ± 13 sec**

Modified a table from ***Serruys et al. State-of-the art EuroIntervention 2023;18(16):e1307-e1327.***

Photon Counting Detector is a Quantum Leap in the MSCT technology

ECG–synchronized ultra-high-resolution photon counting CT: maximum resolution of 0.11 mm

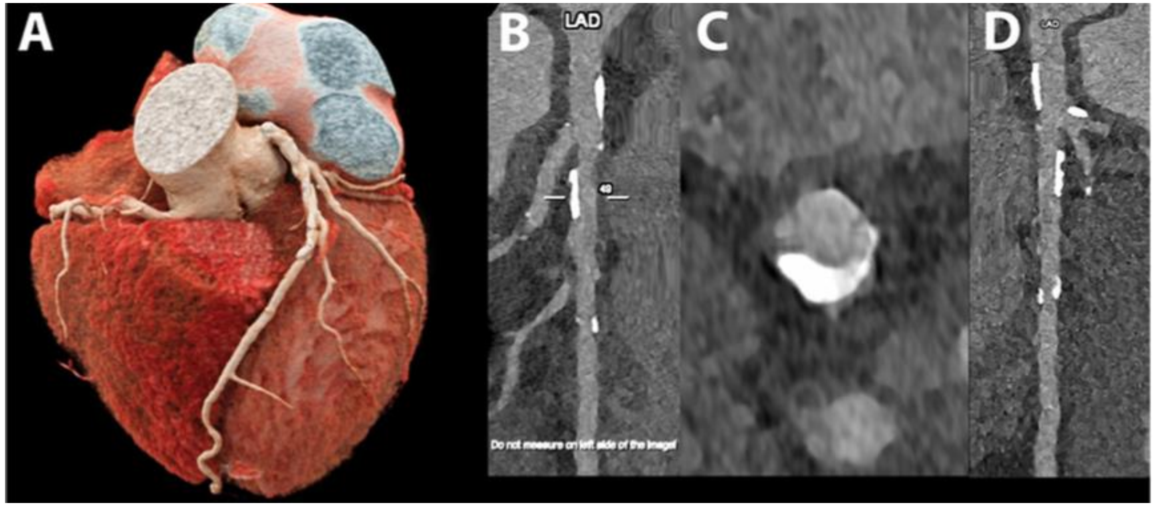

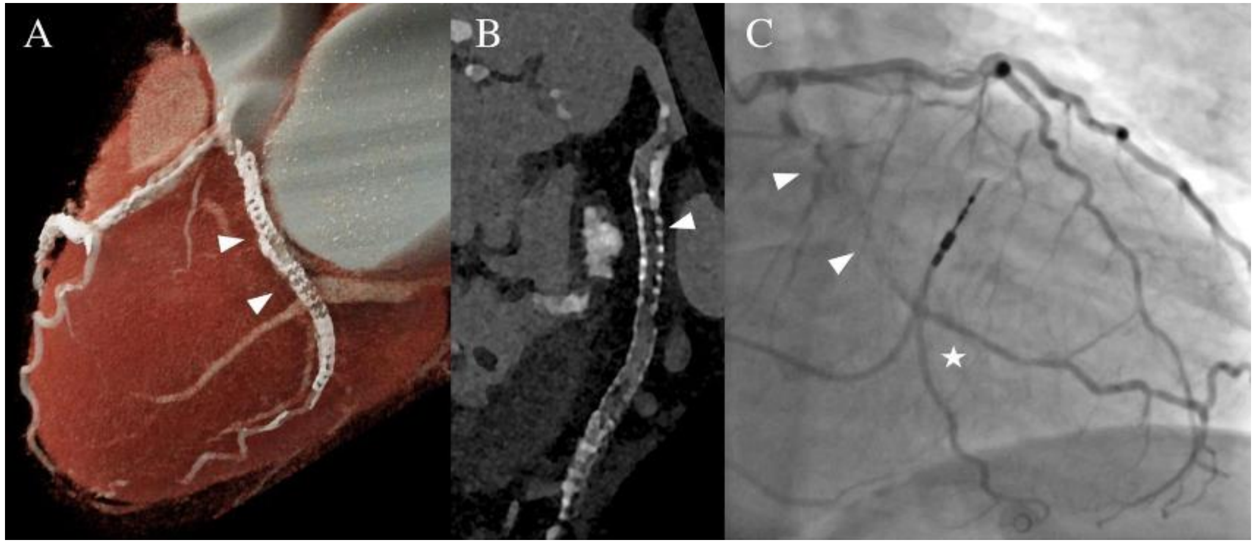

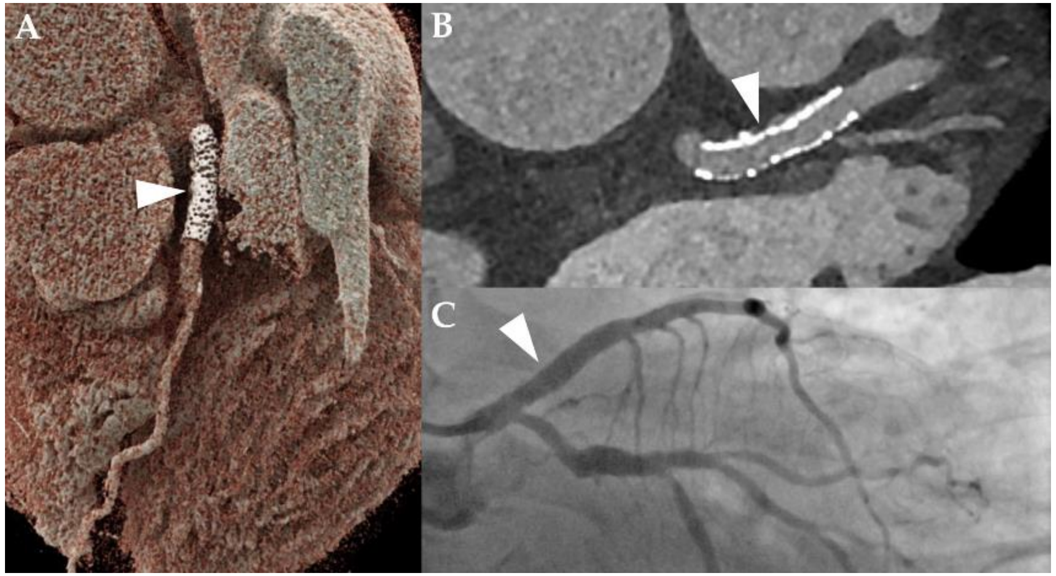

Hagar et al. European Radiology 2024

Meloni et al. J Cardiovasc Dev Dis 2023;10(9):363

Photon-counting CT will be another revolution and may enable the evaluation of calcification and stented segment…maximal resolution…111 microns

Radiology

ORIGINAL RESEARCH • CARDIAC IMAGING

Ultrahigh-Spatial-Resolution Photon-counting Detector CT Angiography of Coronary Artery Disease for Stenosis Assessment

Moritz C. Halfmann, MD • Stefanie Bockius, MD • Tilman Emrich, MD • Michaela Hell, MD • U. Joseph Schoepf, MD • Gerald S. Laux, MD • Larissa Kavermann, MD • Dirk Graafen, MD • Tomasso Gori, MD, PhD • Yang Yang, MD • Roman Kloeckner, MD • Pál Maurovich-Horvat, MD, PhD • Jens Ricke, MD • Lukas Müller, MD • Akos Varga-Szemes, MD, PhD • Nicola Fink, MD

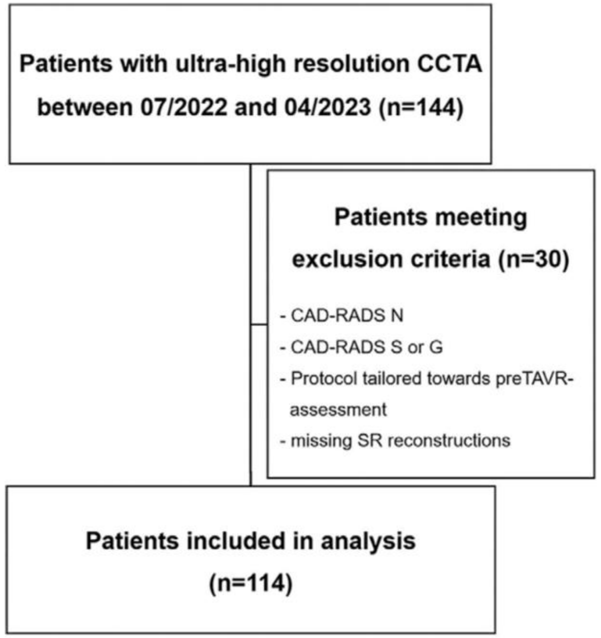

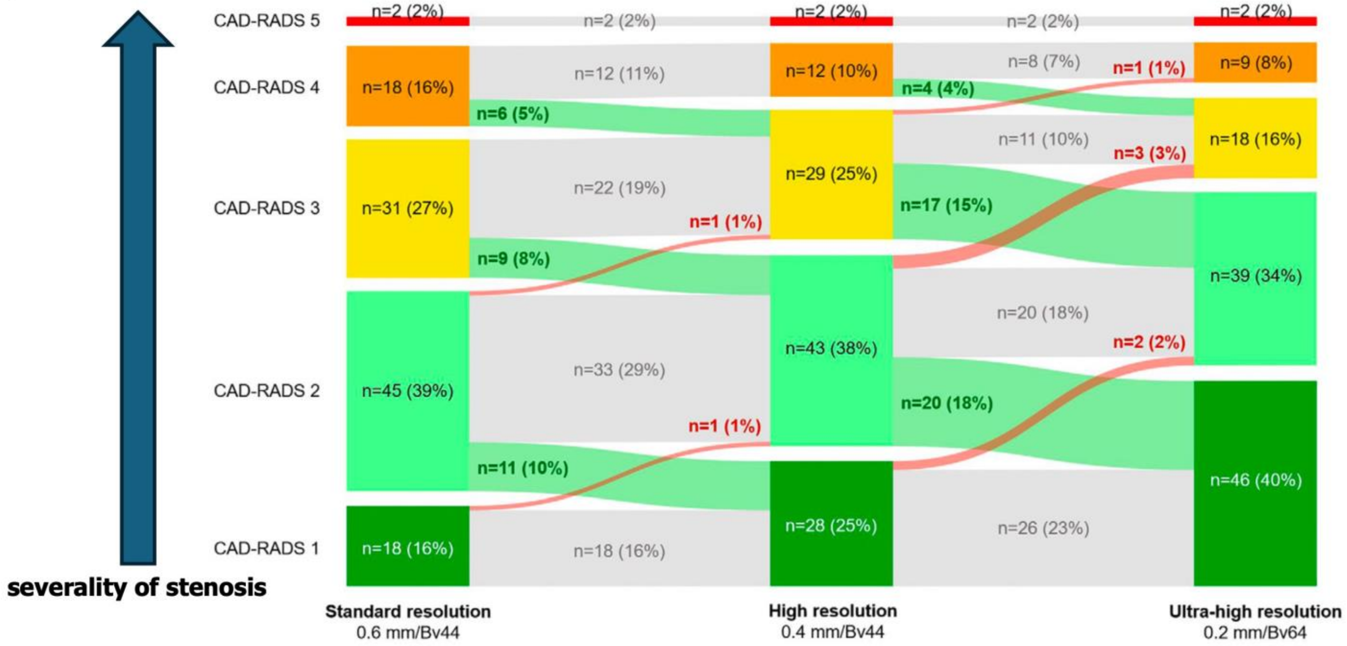

Photon counting CCTA led to reclassification to a lower category with the Coronary Artery Disease Reporting and Data System (CAD-RADS) in 54.4% of patients (62 of 114).

-> Conventinal CCTA may be overestimating stenosis

Radiology 2024 Vol. 310 Issue 2

Conclusion

- **AI is enabling the precise identification of coronary segments and the severity of stenosis using solely coronary angiography.**

- **Various software solutions have demonstrated their efficacy in physiology assessments based on angiography.**

- **CTCA is a powerful imaging tool in assessing anatomy (e.g. stenosis, plaque volume) and physiology.**

- **AI-enabled software for assessment of stenosis and plaque are already available. Advances in photon-counting CT could enhance diagnostic capabilities further.**